# OBSERVATIONAL CONSTRAINTS ON THE NATURE OF DARK ENERGY: FIRST COSMOLOGICAL RESULTS FROM THE ESSENCE SUPERNOVA SURVEY

W. M. Wood-Vasey,[1] G. Miknaitis,[2] C. W. Stubbs,[1,3] S. Jha,[4,5] A. G. Riess,[6,7] P. M. Garnavich,[8]
R. P. Kirshner,[1] C. Aguilera,[9] A. C. Becker,[10] J. W. Blackman,[11] S. Blondin,[1] P. Challis,[1]
A. Clocchiatti,[12] A. Conley,[13] R. Covarrubias,[10] T. M. Davis,[14] A. V. Filippenko,[4]
R. J. Foley,[4] A. Garg,[1,3] M. Hicken,[1,3] K. Krisciunas,[8,15] B. Leibundgut,[16]
W. Li,[4] T. Matheson,[17] A. Miceli,[10] G. Narayan,[1,3] G. Pignata,[12]
J. L. Prieto,[18] A. Rest,[9] M. E. Salvo,[11] B. P. Schmidt,[11]
R. C. Smith,[9] J. Sollerman,[14,19] J. Spyromilio,[16]
J. L. Tonry,[20] N. B. Suntzeff,[9,15] AND A. Zenteno[9]

## ABSTRACT

We present constraints on the dark energy equation-of-state parameter, $w = P/(\rho c^2)$, using 60 SNe Ia from the ESSENCE supernova survey. We derive a set of constraints on the nature of the dark energy assuming a flat universe. By including constraints on $(\Omega_M, w)$ from baryon acoustic oscillations, we obtain a value for a static equation-of-state parameter $w = -1.05^{+0.13}_{-0.12}$ (stat 1 $\sigma$) $\pm 0.13$ (sys) and $\Omega_M = 0.274^{+0.033}_{-0.020}$ (stat 1 $\sigma$) with a best-fit $\chi^2$/dof of 0.96. These results are consistent with those reported by the Supernova Legacy Survey from the first year of a similar program measuring supernova distances and redshifts. We evaluate sources of systematic error that afflict supernova observations and present Monte Carlo simulations that explore these effects. Currently, the largest systematic with the potential to affect our measurements is the treatment of extinction due to dust in the supernova host galaxies. Combining our set of ESSENCE SNe Ia with the first-results Supernova Legacy Survey SNe Ia, we obtain a joint constraint of $w = -1.07^{+0.09}_{-0.09}$ (stat 1 $\sigma$) $\pm 0.13$ (sys), $\Omega_M = 0.267^{+0.028}_{-0.018}$ (stat 1 $\sigma$) with a best-fit $\chi^2$/dof of 0.91. The current global SN Ia data alone rule out empty ($\Omega_M = 0$), matter-only $\Omega_M = 0.3$, and $\Omega_M = 1$ universes at >4.5 $\sigma$. The current SN Ia data are fully consistent with a cosmological constant.

*Subject headings:* cosmological parameters — cosmology: observations — supernovae: general

*Online material:* color figures

## 1. INTRODUCTION: SUPERNOVAE AND COSMOLOGY

We report on the analysis of 60 Type Ia supernovae (SNe Ia) discovered in the course of the ESSENCE program (Equation of State: SupErNovae trace Cosmic Expansion; an NOAO Survey Program) from 2002 through 2005. The aim of ESSENCE is to measure the history of cosmic expansion over the past 5 billion years with sufficient precision to distinguish whether the dark energy is different from a cosmological constant at the $\sigma_w = \pm 0.1$ level. Here we present our first results and show that we are well on our way toward that goal. Our present data are fully consistent with a $w = -1$, flat universe, and our uncertainty in $w$, the parameter that describes the cosmic equation of state, analyzed in the way we outline here, will shrink below 0.1 for models of constant $w$ as the ESSENCE program is completed. Other approaches to using the luminosity distances have been suggested to constrain possible cosmological models. We here provide the ESSENCE observations in a convenient form suitable for testing a variety of models.[21]

As reported in a companion paper (Miknaitis et al. 2007), ESSENCE is based on a supernova search carried out with the 4 m Blanco Telescope at the Cerro Tololo Inter-American Observatory (CTIO) with the prime-focus MOSAIC II 64 Megapixel CCD camera. Our search produces densely sampled *R*-band and *I*-band light curves for supernovae in our fields. As described by Miknaitis et al. (2007), we optimized the search to provide the best constraints on $w$, given fixed observing time and the properties of both the MOSAIC II camera and the CTIO 4 m

[1] Harvard-Smithsonian Center for Astrophysics, Cambridge, MA 02138; wmwood-vasey@cfa.harvard.edu.

[2] Fermilab, Batavia, IL 60510-0500.

[3] Department of Physics, Harvard University, Cambridge, MA 02138.

[4] Department of Astronomy, University of California, Berkeley, CA 94720-3411.

[5] Kavli Institute for Particle Astrophysics and Cosmology, Stanford Linear Accelerator Center, MS 29, Menlo Park, CA 94025.

[6] Space Telescope Science Institute, Baltimore, MD 21218.

[7] Johns Hopkins University, Baltimore, MD 21218.

[8] Department of Physics, University of Notre Dame, Notre Dame, IN 46556-5670.

[9] Cerro Tololo Inter-American Observatory, National Optical Astronomy Observatory, Casilla 603, La Serena, Chile.

[10] Department of Astronomy, University of Washington, Seattle, WA 98195-1580.

[11] Research School of Astronomy and Astrophysics, Australian National University, Mount Stromlo and Siding Spring Observatories, Weston Creek PO 2611, Australia.

[12] Pontificia Universidad Católica de Chile, Departamento de Astronomía y Astrofísica, Casilla 306, Santiago 22, Chile.

[13] Department of Astronomy and Astrophysics, University of Toronto, Toronto, ON M5S 3H4, Canada.

[14] Dark Cosmology Centre, Niels Bohr Institute, University of Copenhagen, DK-2100 Copenhagen, Denmark.

[15] Department of Physics, Texas A&M University, College Station, TX 77843-4242.

[16] European Southern Observatory, D-85748 Garching, Germany.

[17] National Optical Astronomy Observatory, Tucson, AZ 85719-4933.

[18] Department of Astronomy, Ohio State University, Columbus, OH 43210.

[19] Department of Astronomy, Stockholm University, AlbaNova, 10691 Stockholm, Sweden.

[20] Institute for Astronomy, University of Hawaii, Honolulu, HI 96822.

[21] See http://www.ctio.noao.edu/essence/.

telescope. Spectra from a variety of large telescopes, including Keck, VLT, Gemini, and Magellan, allow us to determine supernova types and redshifts. We have paid particular attention to the central problems of calibration and systematic errors that, on completion of the survey in 2008, will be more important to the final precision of our cosmological inferences than statistical sampling errors for about 200 objects.

This first cosmological report from the ESSENCE survey derives some properties of dark energy from the sample presently in hand, which is still small enough that the statistics of the sample size make a noticeable contribution to the uncertainty in dark energy properties. But our goal is to set out the systematic uncertainties in a clear way so that these are exposed to view and so that we can concentrate our efforts where they will have the most significant effect. To infer luminosity distances to the ESSENCE supernovae over the redshift interval 0.15–0.70, we employ the relations developed for SNe Ia at low redshift (Jha et al. 2007 and references therein) among their light-curve shapes, colors, and intrinsic luminosities. The expansion history from $z \approx 0.7$ to the present provides leverage to constrain the equation-of-state parameter for the dark energy as described below.

In § 1 we sketch the context of the ESSENCE program. In § 2 we show from a set of simulated light curves that this particular implementation of light-curve analysis is consistent, with the same cosmology emerging from the analysis as was used to construct the samples, and that the statistical uncertainty we ascribe to the inference of the dark energy properties is also correctly measured. This modeling of our analysis chain gives us confidence that the analysis of the actual data set is reliable and its uncertainty is correctly estimated. Section 3 delineates the systematic errors we confront, estimates their present size, and indicates some areas where improvement can be achieved. Section 4 describes the sample and provides the estimates of dark energy properties using the ESSENCE sample. The conclusions of this work are given in § 5.

## 1.1. *Context*

Supernovae have been central to cosmological measurements from the very beginning of observational cosmology. Shapley (1919) employed supernovae against the "island universe" hypothesis, arguing that objects such as SN 1885A in the Andromeda Nebula would have $M = -16$ mag, which was "out of the question." Edwin Hubble noted "a mysterious class of exceptional novae which attain luminosities that are respectable fractions of the total luminosities of the systems in which they appear" (Hubble 1929). These extrabright novae were dubbed "supernovae" by Baade & Zwicky (1934). Minkowski (1941) divided them into two classes based on their spectra: Type I supernovae (SNe I) have no hydrogen lines, while Type II supernovae (SNe II) show H$\alpha$ and other hydrogen lines.

The high luminosity and observed homogeneity of the first handful of SN I light curves prompted Wilson (1939) to suggest that they be employed for fundamental cosmological measurements, starting with time dilation of their characteristic rise and fall to distinguish true cosmic expansion from "tired light." After the SN Ib and SN Ic subclasses were separated from the SNe Ia (for a review see Filippenko 1997), this line of investigation has grown more fruitful as techniques of photometry have improved and as the redshift range over which supernovae have been well observed and confirmed to have standard light-curve shapes and luminosities has increased (Rust 1974; Leibundgut et al. 1996; Riess et al. 1997, 2004; Goldhaber et al. 2001; Foley et al. 2005; Hook et al. 2005; Conley et al. 2006; Blondin et al. 2006). Within the uncertainties, the results agree with the predictions of cosmic

expansion and provide a fundamental test that the underlying assumption of an expanding universe is correct.

Evidence for the homogeneity of SNe Ia comes from their small scatter in the Hubble diagram. Kowal (1968) compiled data for the first well-populated Hubble diagram of SNe I. The $1 \sigma$ scatter about the Hubble law was 0.6 mag, but Kowal presciently speculated that distances to individual supernovae might eventually be known to 5%–10% and suggested that "[i]t may even be possible to determine the second-order term in the redshift-magnitude relation when light curves become available for very distant supernovae."

Precise distances to SNe Ia enable tests for the linearity of the Hubble law and provide evidence for local deviations from the local Hubble flow, attributed to density inhomogeneities in the local universe (Riess et al. 1995, 1997; Zehavi et al. 1998; Bonacic et al. 2000; Radburn-Smith et al. 2004; Jha et al. 2007). While SN Ia cosmology is not dependent on the value of $H_0$, it is sensitive to deviations from a homogeneous Hubble flow, and these regional velocity fields may limit our ability to estimate properties of dark energy, as emphasized by Hui & Greene (2006) and Cooray & Caldwell (2006). Whether the best strategy is to map the velocity inhomogeneities thoroughly or to skip over them by using a more distant low-redshift sample remains to be demonstrated. We have used a lower limit of redshift $z > 0.015$ in constructing our sample of SNe Ia.

The utility of SNe Ia as distance indicators results from the demonstration that the intrinsic brightness of each SN Ia is closely connected to the shape of its light curve. As the sample of well-observed SNe Ia grew, some distinctly bright and faint objects were found. For example, SN 1991T (Filippenko et al. 1992b; Phillips et al. 1992) and SN 1991bg (Filippenko et al. 1992a; Leibundgut et al. 1993) were of different luminosity, and their light curves were not the same either. The possible correlation of the shapes of supernova light curves with their luminosities had been explored by Pskovskii (1977). More homogeneous photometry from CCD detectors, more extreme examples from larger samples, and more reliable distance estimators enabled Phillips (1993) to establish the empirical relation between light-curve shapes and supernova luminosities. The Calán-Tololo sample (Hamuy et al. 1996) and the CfA sample (Riess et al. 1999; Jha et al. 2006b) of SNe Ia have been used to improve the methods for using supernova light curves to measure supernova distances. Many variations on Phillips's idea have been developed, including $\Delta m_{15}$ (Phillips et al. 1999), MLCS (Riess et al. 1996; Jha et al. 2007), DM15 (Prieto et al. 2006), stretch (Goldhaber et al. 2001), CMAGIC (Wang et al. 2003), and SALT (Guy et al. 2005, 2007).

These methods are capable of achieving the 10% precision for supernova distances that Kowal (1968) foresaw 40 years ago. In the ESSENCE analysis, we have used a version of the Jha et al. (2007) method called MLCS2k2. We have compared it with the results of the Spectral Adaptive Lightcurve Template (SALT; Guy et al. 2005) light-curve fitter used by the SNLS (Astier et al. 2006, hereafter A06). This comparison provides a test: if the two approaches do not agree when applied to the same data, they cannot both be correct. As shown in § 2, SALT and this version of MLCS2k2, with our preferred extinction prior, are in excellent accord when applied to the same data. While gratifying, this agreement does not prove that they are both correct. Moreover, as described in § 4, the cosmological results depend somewhat on the assumptions about SN host galaxy extinction that are employed. This has been an ongoing problem in supernova cosmology. The work of Lira (1995) demonstrated the empirical fact that although SNe Ia have a range of colors at

maximum light, they appear to reach the same intrinsic color about 30–90 days past maximum light, independent of light-curve shape.

Riess et al. (1996) used dereddened SN Ia data to show that intrinsic color differences exist near maximum light, with fainter SNe Ia appearing redder than brighter objects, and then used this information to construct an absorption-free Hubble diagram. Given a good set of observations in several bands, the reddening for individual supernovae can then be determined and the general relations between supernova luminosity and the light-curve shapes in many bands can be established (Hamuy et al. 1996; Riess et al. 1999; Phillips et al. 1999). The initial detections of cosmic acceleration employed either these individual absorption corrections (Riess et al. 1998) or a full-sample statistical absorption correction (Perlmutter et al. 1999). Finding the best approach to this problem, whether by shifting observations to the infrared, limiting the sample to low-extinction cases, or making other restrictive cuts on the data, is an important area for future work. Some ways to explore this issue are sketched in § 4.

Kowal (1968) recognized that second-order terms in cosmic expansion might be measured with supernovae once the precision and redshift range grew sufficiently large. More direct approaches with the *Hubble Space Telescope* (*HST*) were imagined by Colgate (1979) and Tammann (1979). Tammann anticipated that *HST* photometry of SNe Ia at $z \approx 0.5$ would lead to a direct determination of cosmic deceleration and that the time dilation of SN Ia light curves would be a fundamental test of the expansion hypothesis. Early attempts at high-redshift supernova detection were undertaken by a Danish group in 1986–1988 through the European Southern Observatory (ESO) 1.5 m telescope at La Silla Observatory. Their cyclic CCD imaging of the search fields used image registration, convolution and subtraction, and real-time data analysis (Hansen et al. 1987). Alas, the rate of SNe Ia in their fields was lower than they had anticipated, and only one SN Ia, SN 1988U, was discovered and monitored in 2 years of effort (Hansen et al. 1987; Norgaard-Nielsen et al. 1989). More effective searches by the Lawrence Berkeley National Laboratory (LBNL) group exploiting larger CCD detectors and sophisticated detection software showed that this approach could be made practical and be used to find significant numbers of high-redshift SNe Ia (Perlmutter et al. 1995).

By 1995, two groups, the LBNL-based Supernova Cosmology Project (SCP) and the High-Z Supernova Search Team (HZT; Schmidt et al. 1998), were working in this field. The first SN Ia cosmology results using seven high-redshift SNe Ia (Perlmutter et al. 1997) found a universe consistent with $\Omega_M = 1$, but subsequent work by the SCP (Perlmutter et al. 1998) and by the HZT (Garnavich et al. 1998) revised this initial finding to favor a lower value of $\Omega_M$. At the 1998 January meeting of the American Astronomical Society both teams reported that the SN Ia results favored a universe that would expand without limit, but at that time neither team claimed that the universe was accelerating. The subsequent publication of stronger results based on larger samples by the HZT (Riess et al. 1998) and by the SCP (Perlmutter et al. 1999) provided a surprise. The supernova data showed that SNe Ia at $z \approx 0.5$ were about 0.2 mag dimmer than expected in an open universe and pointed firmly at an accelerating universe (for first-hand accounts, see Overbye 1999, p. 426; Riess 2000; Filippenko 2001; Kirshner 2002; Perlmutter 2003; reviews are given by, e.g., Leibundgut 2001; Filippenko 2004, 2005b).

The supernova route to cosmological understanding continues to improve. One source of uncertainty has been the small sample of very well observed low-redshift supernovae (Hamuy et al. 1996; Riess et al. 1999). The most recent contribution is the summary of CfA data obtained in 1997–2001 (Jha et al. 2006b), but significantly enhanced samples from the CfA (Hicken et al. 2006), the Katzman Automatic Imaging Telescope (KAIT; Li et al. 2000; Filippenko et al. 2001; Filippenko 2005a), the Carnegie SN Program (Hamuy et al. 2006), the Nearby Supernova Factory (Wood-Vasey et al. 2004; Copin et al. 2006), and the Sloan Digital Sky Survey II Supernova Survey (SDSS-II; Frieman et al. 2004; Dilday et al. 2005) are forthcoming. As the low-$z$ sample approaches 200 objects, the size of the sample will cease to be a source of statistical uncertainty for the determination of cosmological parameters. As described in § 3, systematic errors of calibration and $K$-correction will ultimately impose the limits to understanding dark energy's properties, and we are actively working to improve these areas (Stubbs & Tonry 2006).

Some of the potential sources of systematic error in the high-$z$ sample have been examined. The fundamental assumption is that distant SNe Ia can be analyzed using the methods developed for the low-$z$ sample. Since nearby samples show that the SNe Ia in elliptical galaxies have a different distribution in luminosity than the SNe Ia in spirals (Hamuy et al. 2000; Howell 2001; Gallagher et al. 2005; Neill et al. 2006; Sullivan et al. 2006b), morphological classification of the distant sample may provide some useful clues to help improve the cosmological inferences (Williams et al. 2003). For example, Sullivan et al. (2003) showed that restricting the SCP sample to SNe Ia in elliptical galaxies gave identical cosmological results to the complete sample, which is principally in spiral galaxies. The possibility of gray dust raised by Aguirre (1999a, 1999b) was examined by Riess et al. (2000) and Nobili et al. (2005) through infrared observations of high-$z$ supernovae and was put to rest by the very high redshift observations of Riess et al. (2004, 2007). Improved methods for handling the vexing problems of absorption by dust have been developed by Knop et al. (2003) and Jha et al. (2007). These questions are described in more detail in § 3.3.

The question of whether distant supernovae have spectra that are the same as those of nearby supernovae has been investigated by Coil et al. (2000), Lidman et al. (2005), Matheson et al. (2005), Hook et al. (2005), Howell et al. (2005), and Blondin et al. (2006). Foley et al. (2005) then confirmed that spectra of distant SNe Ia evolve over the lifetime of the SN Ia in the same way as those of nearby SNe Ia. In all cases, the evidence points toward nearby SNe Ia behaving in the same way as distant ones, bolstering confidence in the initial results. This observed consistency does not mean that the samples are identical, only that the variations between the nearby and distant samples are successfully accounted for by the methods currently in hand. We do not know whether this will continue to be the case as future investigations press for more stringent limits on cosmological parameters (Albrecht et al. 2006).

The highest redshift SN Ia data (Riess et al. 2004, 2007) show the qualitative signature expected from a mixed dark energy/dark matter cosmology. Specifically, they show that cosmic deceleration due to dark matter preceded the current era of cosmic acceleration produced by dark energy. The sign of the observed effect on supernova apparent magnitudes reverses: SNe Ia at $z \approx 0.5$ appear 0.2 mag dimmer than expected in a coasting cosmology, but the very distant supernovae whose light comes from $z > 1$ appear brighter than they would in that cosmology. By itself, this turnover is a very encouraging sign that supernova cosmology does not founder on gray dust or even on a simple evolution of supernova properties with cosmic epoch. As part of this analysis, Riess et al. (2004) constructed the "gold" sample of high-$z$ and low-$z$ supernovae whose observations met reasonable criteria for inclusion in an analysis of all of the published light curves and

spectra using a uniform method of deriving distances from the light curves.

The analysis of the gold sample provided an estimate of the time derivative of the equation-of-state parameter, $w$, for dark energy. These observations are very important conceptually because the simplest fact about the cosmological constant as a candidate for dark energy is that it should be constant with redshift (i.e., $w' = dw/dz = 0$). The observations are consistent with a constant dark energy over the redshift range out to $z \approx 1.6$. Other forms of dark energy might satisfy the observed constraints, but this observational test is one that the cosmological constant could have failed. The next definitive advance in our understanding of $w$ came from the SNLS analysis of 71 SNe Ia, which constrained constant models of $w$ to $w = -1.023 \pm 0.09$ (stat) $\pm 0.054$ (sys) and was consistent with a flat universe dominated by a cosmological constant (A06).

In the analysis of the ESSENCE data presented in § 4, we use the supernova data to constrain the properties of $w$, as first carried out by White (1998) and Garnavich et al. (1998). This parameterization of dark energy by $w$ is not the only possible approach. A more detailed approach is to compare the observational data to a specific model and, for example, try to reconstruct the dark energy scalar field potential (see, e.g., Li et al. 2007). A more agnostic view is that we are simply measuring the expansion history of the universe, and a kinematic description of that history in terms of expansion rate, acceleration, and jerk (Riess et al. 2004, 2007; Rapetti et al. 2007) covers the facts without assuming anything about the nature of dark energy.

The ESSENCE project was conceived to tighten the constraints on dark energy at $z \approx 0.5$ to reveal any discrepancy between the observations and the leading candidate for dark energy, the cosmological constant. A simple way to express this is that we aim for a 10% uncertainty in the value of $w$. This program is similar to the approach of the SNLS being carried out at the Canada-France-Hawaii Telescope, and we compare our methods and results to theirs (Guy et al. 2005; A06) at several points in the analysis below.

The SNLS has taken the admirable step of publishing their light curves online and making the code of their light-curve fitting program, SALT, available for public inspection and use.[22] Making the light curves public, as was done for the results of the HZT and its successors (Riess et al. 1998; Tonry et al. 2003; Barris et al. 2004; Krisciunas et al. 2005; Clocchiatti et al. 2006), by Knop et al. (2003), by Riess et al. (2004, 2007) for the very high redshift *HST* supernova program, and for the low-$z$ data of Hamuy et al. (1996), Riess et al. (1999), and Jha et al. (2006b), provides the opportunity for others to perform their own analysis of the results. In addition to exploring a variety of approaches to analyzing our own SN Ia observations, in § 4 we show the first joint constraints from ESSENCE and the first year of SNLS, as well as some joint constraints derived from combining these with the Riess et al. (2004) gold sample.

## 2. LUMINOSITY DISTANCE DETERMINATION

The physical quantities of interest in our cosmological measurements are the redshifts and distances to a set of spacetime points in the universe. The redshifts come from spectra and the luminosity distances, $D_L$, come from the observed flux of the supernova combined with our understanding of SN Ia light curves from nearby objects.

Extracting a luminosity distance to a supernova from observations of its light curve necessitates a number of assumptions.

We use the observations of nearby SNe Ia to establish the relations between color, light-curve shape in multiple bands, and peak luminosity. These nearby observations attain high signal-to-noise ratios (S/Ns), and the nearby objects can be observed in more passbands (including infrared) than faint, distant objects. We assume that the resulting method of converting light curves to luminosity distances applies at all redshifts. The observed spectral uniformity of supernovae over a range of redshift (Coil et al. 2000; Lidman et al. 2005; Hook et al. 2005; Blondin et al. 2006) supports this approach. We assume that $R_V$, the ratio of extinction in the $V$ band to the color excess $E(B - V)$, is independent of redshift. In § 3.3 we test the potential systematic effect of departures from this assumption. We adopt an astrophysically sensible prior distribution of host galaxy extinction properties, with a redshift dependence that is derived from the simulations we present below.

Our approach is to conduct comprehensive simulations of the ESSENCE data and analysis. As described by Miknaitis et al. (2007), we use this same approach to explore our photometric performance. For the aspects of our analysis that are "downstream" of the light-curve generation, we generate sets of synthetic light curves and subject them to our analysis pipeline. In this way we can test the performance of our distance-fitting tools, and by exaggerating various systematic errors (zero-point offsets, etc.), we can assess the impact of these effects on our determination of $w$.

### 2.1. *Extracting Luminosity Distances from Light Curves: Distance Fitters*

We use the MLCS2k2 method of Jha et al. (2007) as the primary tool to derive relative luminosity distances to our SNe Ia. For comparison, we also provide the results obtained using the SALT fitter of Guy et al. (2005) on the ESSENCE light curves. SALT was used in the recent cosmological results paper from the SNLS (A06). We provide a consistent and comprehensive set of distances obtained to nearby, ESSENCE, and SNLS supernovae for each luminosity distance fitting technique. The ESSENCE light curves used in this analysis were presented by Miknaitis et al. (2007), and we provide them online, together with our set of previously published light curves for nearby SNe Ia, for the convenience of those interested (see footnote 21). Additional SN Ia light-curve fitting methods will be further explored in future ESSENCE analyses. Understanding the behavior of our distance determination method is critical to our goal of quantifying the uncertainties of our analysis chain.

MLCS2k2 and SALT, as well as the light-curve "stretch" approach used by Perlmutter et al. (1997, 1999), Goldhaber et al. (2001), and Knop et al. (2003), exploit the fact that the rate of decline, the color, and the intrinsic luminosity of SNe Ia are correlated. At present we treat SNe Ia as a single-parameter family, and the distance-fitting techniques use multicolor light curves to deduce a luminosity distance and host galaxy reddening for each supernova. Previous papers have shown that the different techniques produce relative luminosity distances that scatter by $\sim 0.10$ mag for an individual SN Ia (e.g., Tonry et al. 2003), but this scatter is uncorrelated with redshift. Consequently, the cosmological results are insensitive to the distance fitting technique. However, as described by Miknaitis et al. (2007), the measurement of the equation-of-state parameter hinges on subtle distortions in the Hubble diagram, so we have undertaken a comprehensive set of simulations to understand potential biases introduced by MLCS2k2. Based on simulations of 10,000 light curves that explored the data quality range spanned by the nearby and ESSENCE light curves, we developed a set of quality thresholds

---

[22] See http://snls.in2p3.fr/conf/release/.

TABLE 1
MLCS2k2 Fit Parameter Quality Cuts

| Fit Parameter | Requirement |
|---|---|
| $\chi_\nu^2$ ........................................ | $\chi_\nu^2 \le 3$ |
| Degrees of freedom................................ | dof $\ge 4$ |
| $\Delta$ ........................................ | $-0.4 \le \Delta \le 1.7$ |
| Time of maximum uncertainty .................. | $T_{max_{err}} \le 2.0$ rest-frame days |
| First observation with S/N > 5 ................. | $\le +4$ days |
| Last observation with S/N > 5 ................. | $\ge +9$ days |

Notes.—See Table 4 for the MLCS2k2 fit parameters used for the cosmological analysis presented in this paper. These selection criteria were derived based on Monte Carlo simulations discussed in § 2.5. The number of degrees of freedom is the number of light-curve points with S/N > 5 minus the four independent MLCS2k2 fit parameters: $m_V$, $\Delta$, $A_V$, and $T_{max}$.

TABLE 2
SALT Fit Parameter Quality Cuts

| Fit Parameter | Requirement |
|---|---|
| $\chi_\nu^2$ ........................................ | $\chi_\nu^2 \le 3$ |
| Degrees of freedom................................ | dof $\ge 5$ |
| Stretch ........................................ | $0.5 \le s < 1.4$ |
| Time of maximum uncertainty .................. | $T_{max_{err}} \le 2.0$ rest-frame days |
| Observations after $B$-band maximum........ | $>1$ |
| First observation with S/N > 5 ................. | $\le +5$ days |

Notes.—See Table 5 for the SALT fit parameters used for the cosmological analysis presented in this paper. These selection criteria were based on A06 with additional sanity checks on the stretch parameter and uncertainty in the time of maximum light. The number of degrees of freedom is the number of light-curve points with S/N > 5 minus the four independent SALT fit parameters: $m_B$, stretch, color, and $T_{max}$.

to require for including SNe Ia in our cosmological analysis. These "cuts" are summarized in Table 1. The fit quality requirements derived from fitting these simulated light curves with the SALT fitter are summarized in Table 2.

The MLCS2k2 approach (Riess et al. 1996, 1998; Jha et al. 2007) to determining luminosity distances uses well-observed nearby SNe Ia to establish a set of light-curve templates in multiple passbands. The parameters $\Delta$ (roughly equivalent to the variation in peak visual luminosity, this parameter characterizes intrinsic color, rate of decline, and peak brightness), $A_V$ (the $V$-band extinction of the supernova light in its host galaxy), and $\mu$ (the distance modulus) are then determined by fitting each multiband set of distant supernova light curves to redshifted versions of these templates. Jha et al. (2007) present results from MLCS2k2 based on nearby SNe Ia. Here we have modified MLCS2k2 for application to both high- and low-redshift SNe Ia. We begin with a rest-frame model of the SN Ia in its host galaxy and then propagate the model light curves through the host galaxy extinction, $K$-correction, and Milky Way extinction to the detector, incorporating the measured passband response (including the atmosphere for ground-based observations). We then fit this model directly to the natural-system observations. This forward-modeling approach has particular advantages in application to the more sparsely sampled (in color and time) data typical of high-redshift SN searches.

The SALT method of Guy et al. (2005), which was used for the SNLS first-results analysis of A06, constructs a fiducial SN Ia template using combined spectral and photometric information, then transforms this template into the rest frame of the SN Ia, and finally calculates a flux, stretch, and generalized color. The color parameter in SALT is notable in that it includes both the intrinsic variation in SN Ia color and the extinction from dust in the host galaxy within a single parameter (in contrast, MLCS2k2 attempts to separate these components of the observed colors for each supernova). While the reddening vector (attenuation vs. color excess) is similar to the SN Ia color versus absolute magnitude relation, the two sources of correlated color and luminosity variation are not identical.

The stretch and color parameters of SALT were used by A06 to estimate luminosity distances by marginalizing over the stretch-luminosity and color-luminosity relationships during the cosmological fit for the full SN Ia sample. Given that the SALT color parameter conflates the two physically distinct phenomena of host galaxy extinction and SN Ia color variation, it is remarkable and perhaps a source of deep insight that this treatment works as well as it does. Because of both survey selection effects and possible demographic shifts in the host environments of SNe Ia, we would not expect that the proportion of reddening from dust

and from intrinsic variation would remain constant with redshift as this approach assumes. However, the SALT/A06 method does seem to work quite well in practice.

### 2.2. Sensitivity to Assumptions about the Host Galaxy Extinction Distribution: Extinction Priors

The best way to treat host galaxy extinction is a serious question for this work and for the field of supernova cosmology. The Bayesian approach we use is detailed in § 3.4. Here we describe simulations that are designed to evaluate the effects of those methods.

There have been four basic approaches to combining reddening measurements with astrophysical knowledge to determine the host galaxy extinction along the line of sight: (1) assume that linear $A_V$ is the natural space for extinction and assume a flat prior (Perlmutter et al. 1999; Knop et al. 2003); (2) use models of the dust distribution in galaxies (Hatano et al. 1998; Commins 2004; Riello & Patat 2005) to model line-of-sight extinction values (Riess et al. 1998, 2004; Tonry et al. 2003); (3) assume that the distribution of host galaxy $A_V$ follows an exponential form (Jha et al. 2007), based on observed distributions of $A_V$ in nearby SNe Ia; and (4) self-calibrate within a set of low-$z$ SNe Ia to obtain a consistent color$+A_V$ relationship and assume that relation for the full set (A06).

Approach 1 assumes the least prior knowledge about the distribution of $A_V$ and produces a Gaussian probability distribution for the fitted luminosity distance. However, this approach weakens the ability to separate intrinsic SN Ia color from $A_V$, resulting in a fit parameter $A_V$ that is a mixture of the two. An $A_V$ that is truly related to the dust extinction should never be negative. The probability prior with $-\infty < A_V < +\infty$ is not the natural range over which to assume a flat distribution; the physically reasonable prior on $A_V$ should be strictly positive.

One approach is to base the prior for absorption on the distribution of dust in galaxies. Theoretical modeling of dust distributions in galaxies, such as that of Hatano et al. (1998), Commins (2004), and Riello & Patat (2005), provides a physically motivated dust distribution. This method represents approach 2 above and is the method we adopt here. In contrast, Jha et al. (2007) empirically derived an exponential $A_V$ distribution from MLCS2k2 fits to nearby SNe Ia by assuming a particular color distribution of SNe Ia. This distribution was derived using the empirical fact that SNe Ia reach a common color about 40 days past maximum light (Lira 1995). They found an exponential distribution of $A_V$,

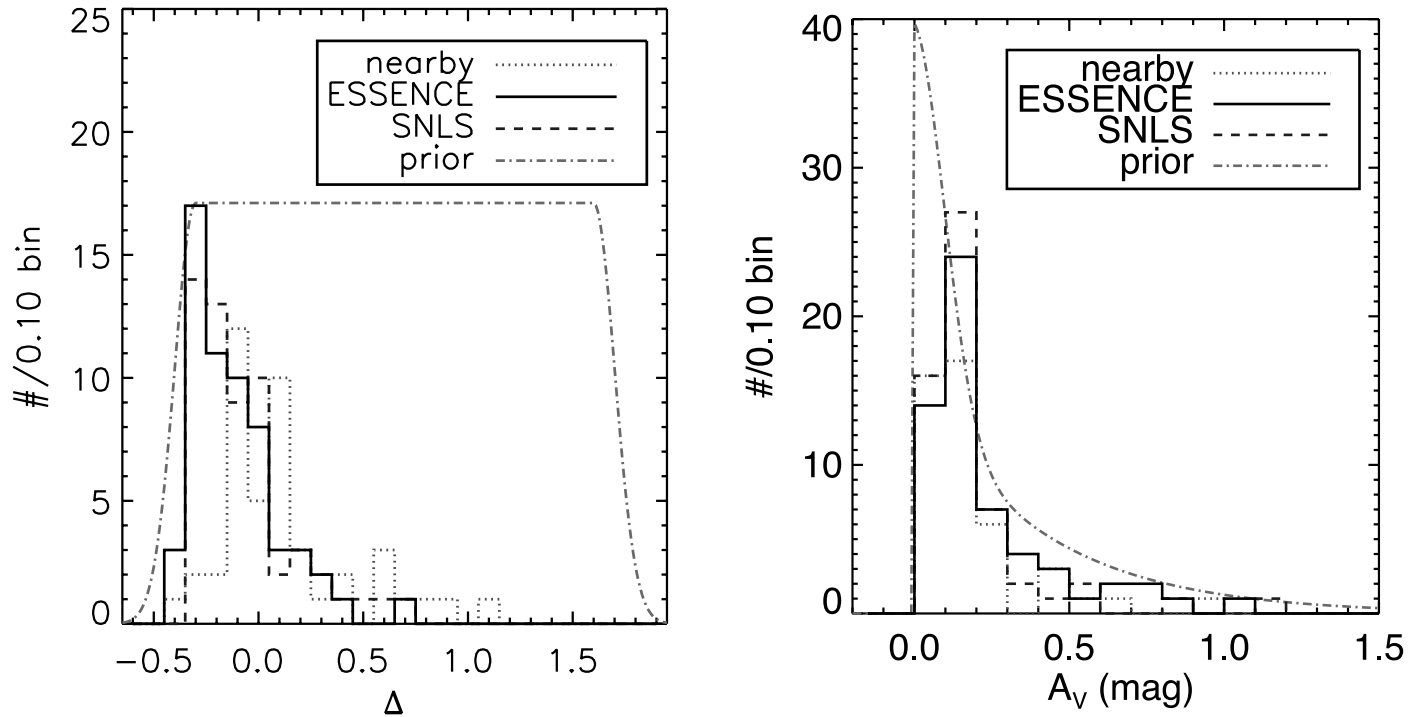$$p(A_V) \propto \exp\left(\frac{-A_V}{\tau}\right), \qquad (1)$$

FIG. 1.—Distribution of the MLCS2k2 light-curve width parameter $\Delta$ and $A_V$ for the MLCS2k2 fits with the glosz prior to the nearby (*dotted line*), ESSENCE (*solid line*), and SNLS (*dashed line*) SNe Ia considered in this paper. The glosz prior (*dot-dashed line*) is shown here for $z = 0$, where it is equivalent to the glos prior. Note that we are mixing two slightly different things in showing the prior with these estimated mean fit parameters. The prior, which directly relates to the mode, is not expected to match the a posteriori mean distribution of the fit parameters. See Fig. 7 for the ESSENCE selection effect as a function of redshift. See Table 4 for the full set of MLCS2k2 light-curve fit results for these SNe Ia. [*See the electronic edition of the Journal for a color version of this figure.*]

where $\tau = 0.46$ mag. Unfortunately, the highest extinction objects drive the tail of this exponential and significantly affect the fit, resulting in a prior sensitive to sample selection, which differs significantly in high-redshift searches compared to the nearby objects studied by Jha et al. (2007).

A06 analyzed the results of the SALT SN Ia light-curve fitter with approach 4 and have systematic sensitivities that are similar to those of approach 1.

We use MLCS2k2 as our main analysis tool. We designate approach 1 the "flatnegav" prior and approach 3 the "default" prior and discuss both of these further in § 3.4. Approach 2 is based on a galactic line-of-sight ("glos") prior on $A_V$:

$$\hat{p}(A_V) \propto \frac{A}{\tau} \exp\left(\frac{-A_V}{\tau}\right) + \frac{2B}{\sqrt{2\pi}\sigma} \exp\left(\frac{-A_V^2}{2\sigma^2}\right), \quad (2)$$

where $A = 1$, $B = 0.5$, $\tau = 0.4$, $\sigma = 0.1$, and $\hat{p}(A_V) \equiv 0$ for $A_V < 0$. This exponential plus one-sided narrow Gaussian glos prior is based on the host galaxy dust models of Hatano et al. (1998), Commins (2004), and Riello & Patat (2005). As described below, we have modeled our selection effects with redshift to adapt the glos prior into the "glosz" prior that is the basis for our analysis. We feel that this approach leverages our best understanding of the effects of extinction and selection.

Figures 1 and 2 show the distribution of the fit parameters and overlay the prior distribution assumed for each of these approaches. Figures 3 and 4 demonstrate that there is no significant residual correlation between distance modulus and the fit parameters using the built-in MLCS2k2 width-luminosity relationship or SALT using the $\alpha$ and $\beta$ parameters from A06. Figure 5 compares the fit distances and extinction/color parameters of the MLCS2k2 glosz and SALT fit results for the ESSENCE, SNLS, and nearby samples. The distribution of

recovered $\Delta$ and $A_V$ match their imposed priors for MLCS2k2 glosz, while the stretch and color fit parameters from SALT show a consistent distribution for the three different sets of SNe Ia.

### 2.3. *ESSENCE Selection Effects and the Motivation for a Redshift-dependent Extinction Prior*

We examined the effect of the survey selection function on the expected demographics of the ESSENCE SNe Ia and explored the interplay between extinction, Malmquist bias, and our observed light curves. To determine the impact of the selection bias, we developed a Monte Carlo simulation of the ESSENCE search. We created a range of supernova light curves that match the properties of the nearby sample, added noise based on statistics from actual ESSENCE photometry, and then fitted the resulting light curves in the same manner that the real events are analyzed. In this way we estimated the impact of subtle biases, although this simulation cannot test for errors in our light-curve model or population drift with redshift.

Based on its low-redshift training set, MLCS2k2 is able to output a finely sampled light curve given a redshift ($z$), distance modulus ($\mu$), light-curve shape parameter ($\Delta$), host extinction ($A_V$), host extinction law ($R_V$), date of rest-frame $B$-band maximum light ($t_0$), Milky Way reddening [$E(B - V)_{\rm MW}$], and the bandpasses of the observations. At a given redshift we calculated a distance modulus, $\mu_{\rm true}$, from the luminosity distance for the standard cosmology ($\Omega_m = 0.3$, $\Omega_\Lambda = 0.7$), and that distance modulus plus an assumed $M_B = -19.5$ mag for SNe Ia set the brightness for our simulated supernovae. Varying the assumed cosmology does not significantly impact the simulation results since we are comparing the input distance modulus with the recovered distance modulus, $\mu_{\rm obs}$, which is independent of the cosmology.
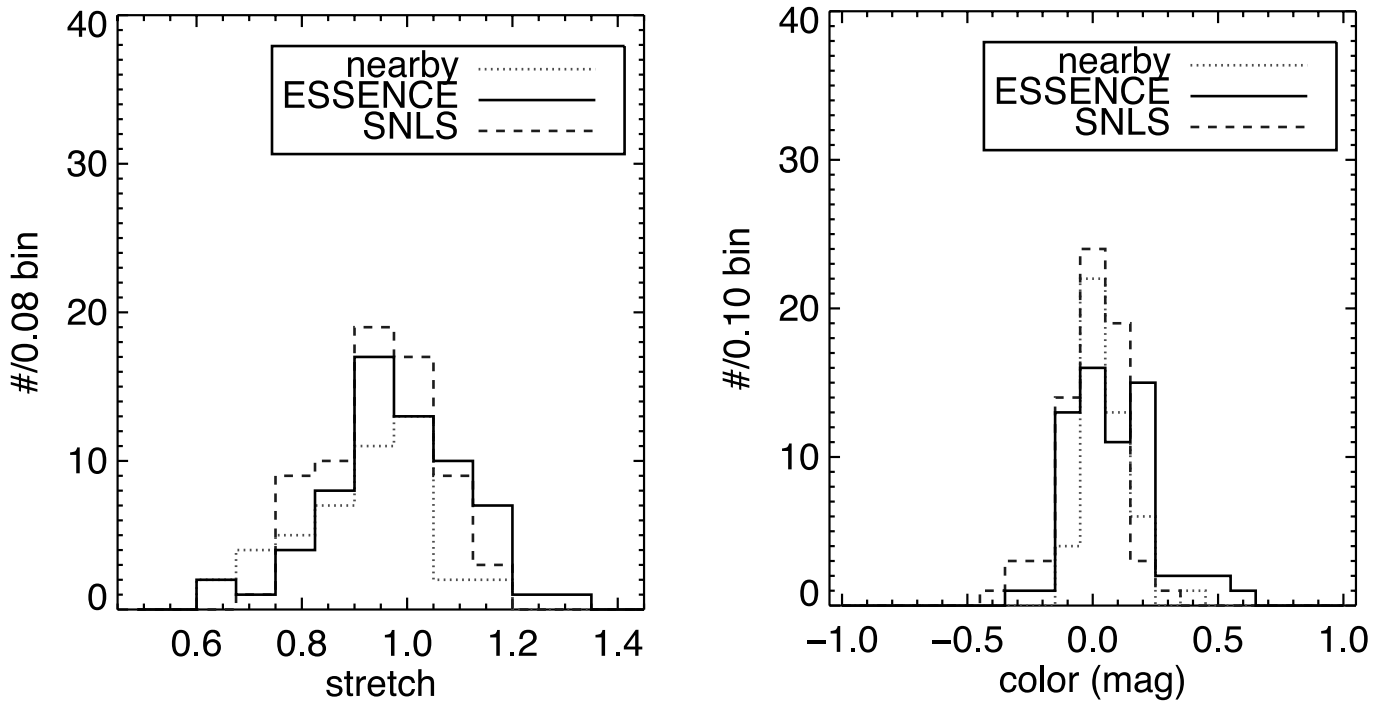
Fig. 2.—Distribution of the SALT light-curve stretch and the SALT estimated color plus extinction (the "$c$" parameter of Guy et al. [2005]; sixth column of Table 5) for the nearby (*dotted line*), ESSENCE (*solid line*), and SNLS (*dashed line*) SNe Ia considered in this paper. The priors for SALT are effectively flat for stretch and color, and SALT quotes minimum $\chi^2$ values instead of the estimated mean parameter values of MLCS2k2. See Table 5 for the full set of SALT light-curve fit results for these SNe Ia. [*See the electronic edition of the Journal for a color version of this figure.*]

At each of a series of fixed redshifts, we created ∼1000 simulated light curves with parameters chosen from random distributions. The light-curve width, $\Delta$, was selected from the Jha et al. (2007) distribution measured from the low-$z$ sample. The $\Delta$ distribution is approximately a Gaussian peaking at $\Delta = -0.15$ with an extended tail out to $\Delta = 1.5$. The host extinction for each simulated event, $A_V$, was selected from either the Jha et al. (2007) distribution (default) estimated from the

local sample or from a "galaxy line-of-sight" estimation (glos). The default distribution was an exponential decay with index 0.46 mag and set to zero for $A_V < 0.0$ mag. The glos distribution is also set to zero for $A_V < 0.0$ mag and combines a narrow Gaussian with an exponential tail for $A_V > 0.0$ mag (see eq. [2]). The extinction law is assumed to be $R_V = 3.1$. The Milky Way reddening [$E(B - V)_{MW}$] distribution was constructed from the Schlegel et al. (1998, hereafter SFD98) reddening maps that
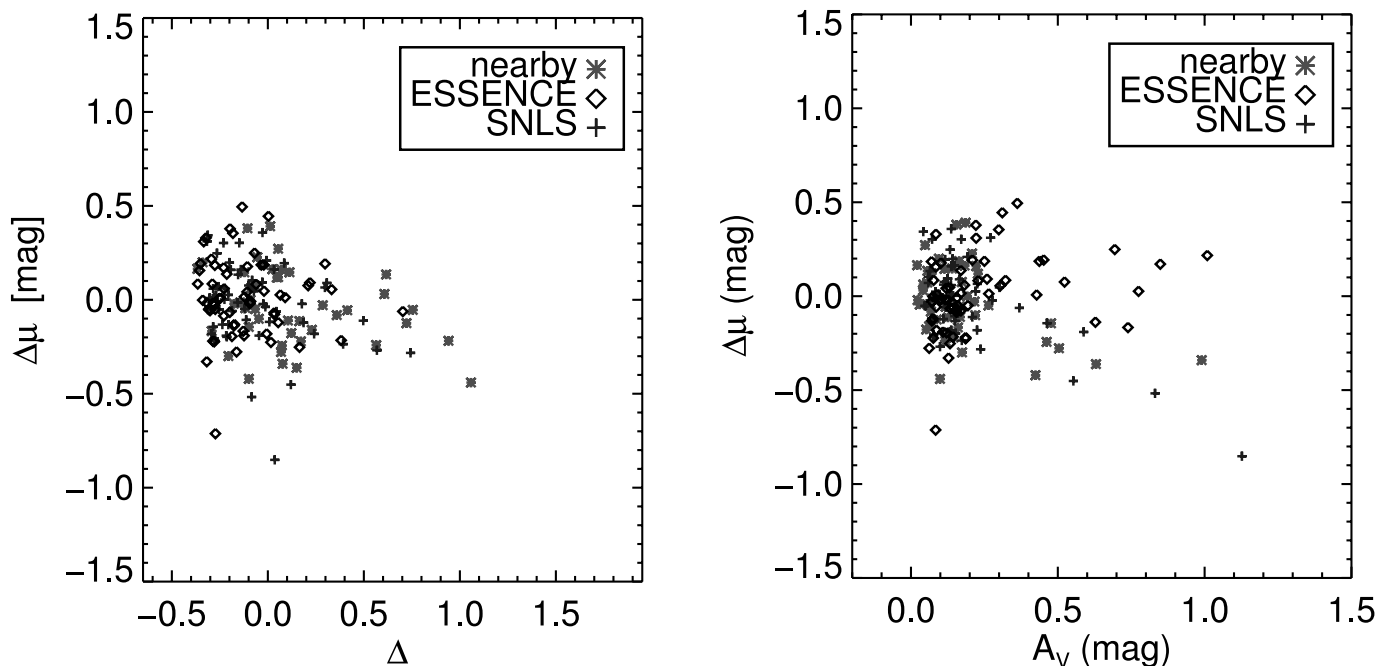


Fig. 3.—Distance modulus ($\mu$) residuals with respect to a $\Lambda$CDM cosmology as a function of the MLCS2k2 glosz fit parameters: $\Delta$ and $A_V$. See Table 4. [*See the electronic edition of the Journal for a color version of this figure.*]
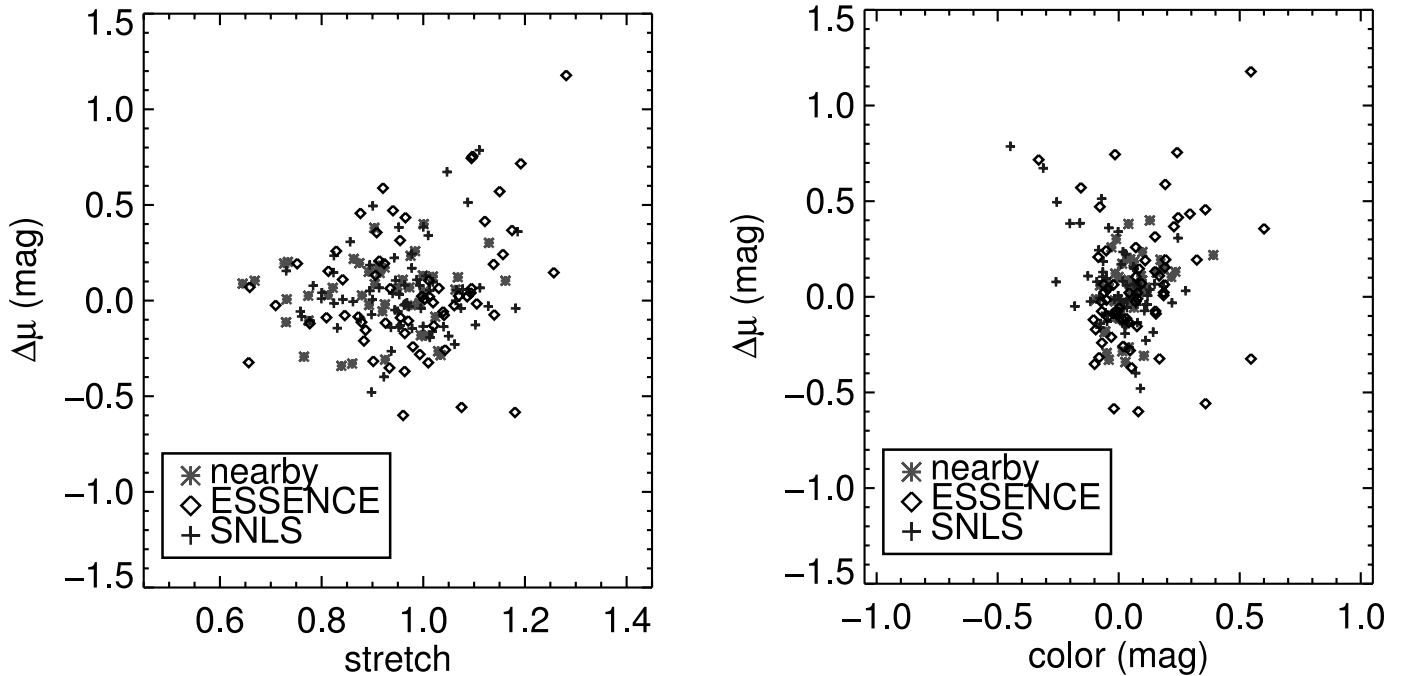
Fig. 4.—Distance modulus ($\mu$) residuals with respect to a $\Lambda$CDM cosmology as a function of the SALT fit parameters: stretch and color. See Table 5. [*See the electronic edition of the Journal for a color version of this figure.*]

cover the ESSENCE fields. $E(B - V)_{\mathrm{MW}}$ was measured for 10,000 random locations in each ESSENCE field, and the reddening was selected from the sum of the histograms (see Fig. 2).

The dates of observation for a simulated SN Ia were based on the actual dates of ESSENCE 4 m observations. An ESSENCE field was chosen at random from the list of monitored fields and a date of maximum, $t_0$, selected to fall randomly between the Modified Julian Date (MJD) of the first and last observation of an observing season. The simulated light curve was then interpolated for only those dates that ESSENCE took images. With each ESSENCE field observation, we estimated the magnitude in $R$ and $I$ that provided a 10 $\sigma$ photometric detection based on the seeing and sky brightness. The S/N for each simulated light-curve point was then scaled from the 10 $\sigma$ detection magnitude, assuming that the noise was dominated by the sky background.

For each date of ESSENCE observation, we have a simulated noiseless magnitude and an estimate of the S/N of the observation. To each simulated observation we added an appropriate random value in flux space selected from a normal distribution with a width corresponding to the predicted S/N.

MLCS2k2 was then used to fit the simulated light curves and provide estimates of $\mu$, $\Delta$, $A_V$, and $t_0$, assuming a fixed $R_V = 3.1$ in the same manner as used for the real light curves. MLCS2k2 required an initial guess of the date of maximum, an estimate achieved by selecting from a normal distribution about the true date with a 1 $\sigma$ width of 2 days. The SFD98 Milky Way reddening was also required in MLCS2k2 and was provided from the true reddening after adding an uncertainty of 10%. Finally, in the real ESSENCE data we discarded supernovae when the MLCS2k2 reduced $\chi^2/$dof indicated a very poor fit. We treated the simulated light curves similarly and dropped events from the sample if the reduced $\chi^2$ exceeded 2.

### 2.3.1. *Deriving an Extinction Prior from the Simulation Results*

Simulated ESSENCE samples were created at a range of redshifts out to $z = 0.70$, and the light curves that passed the detection criteria from the actual ESSENCE search were fitted

with MLCS2k2. The fitting was done with the default prior and the glos prior (with corresponding $A_V$ distributions). The difference between the "true" (input) distance modulus and recovered (fit) distance modulus, $\Delta\mu$, was calculated for each event, and the mean, median, and dispersion for the ensemble were calculated at each redshift. The median $\Delta\mu$ of the simulations was within 0.03 mag for $z < 0.45$, but at higher redshift the simulated supernovae were estimated to be brighter than the input supernovae by more than 0.2 mag. This bias results from the loss of faint events (large $A_V$ and large $\Delta$) from the sample as the distance increases. In a sense, this is a classic Malmquist bias, but here it is caused by an uninformed prior. These results are shown in Figure 6.

The decreasing ability to observe large $A_V$ events as the redshift increases (see Fig. 7) makes it clear that using a single $A_V$ prior for all redshifts is not correct. Because events with large $A_V$ and large $\Delta$ are lost at high redshift due to the magnitude limits of the search, we should adjust the prior as a function of $z$ to account for these predictable losses. Applying redshift-dependent window functions to the basic glos prior provides a much better prior as a function of redshift.

We fit the recovered $A_V$ distributions derived from the simulations, which start with a uniform $A_V$, to a window function based on the error function (integral of a Gaussian), and two parameters describe where that function drops to half its peak value ($A_{1/2}$) and the width of the transition ($\sigma_A$). The window function $W$ has the form

$$W\left(A_V, A_{1/2}, \sigma_A\right) = 1 - \frac{1}{\sqrt{\pi}} \int_{-\infty}^{(A_V - A_{1/2})\sigma_A} e^{-x^2} dx, \quad (3)$$

where $A_{1/2}$ and $\sigma_A$ are functions of $z$ and estimated from the simulations. A similar process was applied to the $\Delta$ distribution, and Table 3 provides the parameters. We embody this prescription in the glosz prior we use for our main MLCS2k2 light-curve fitting. The glosz prior is the glos prior modified by the above
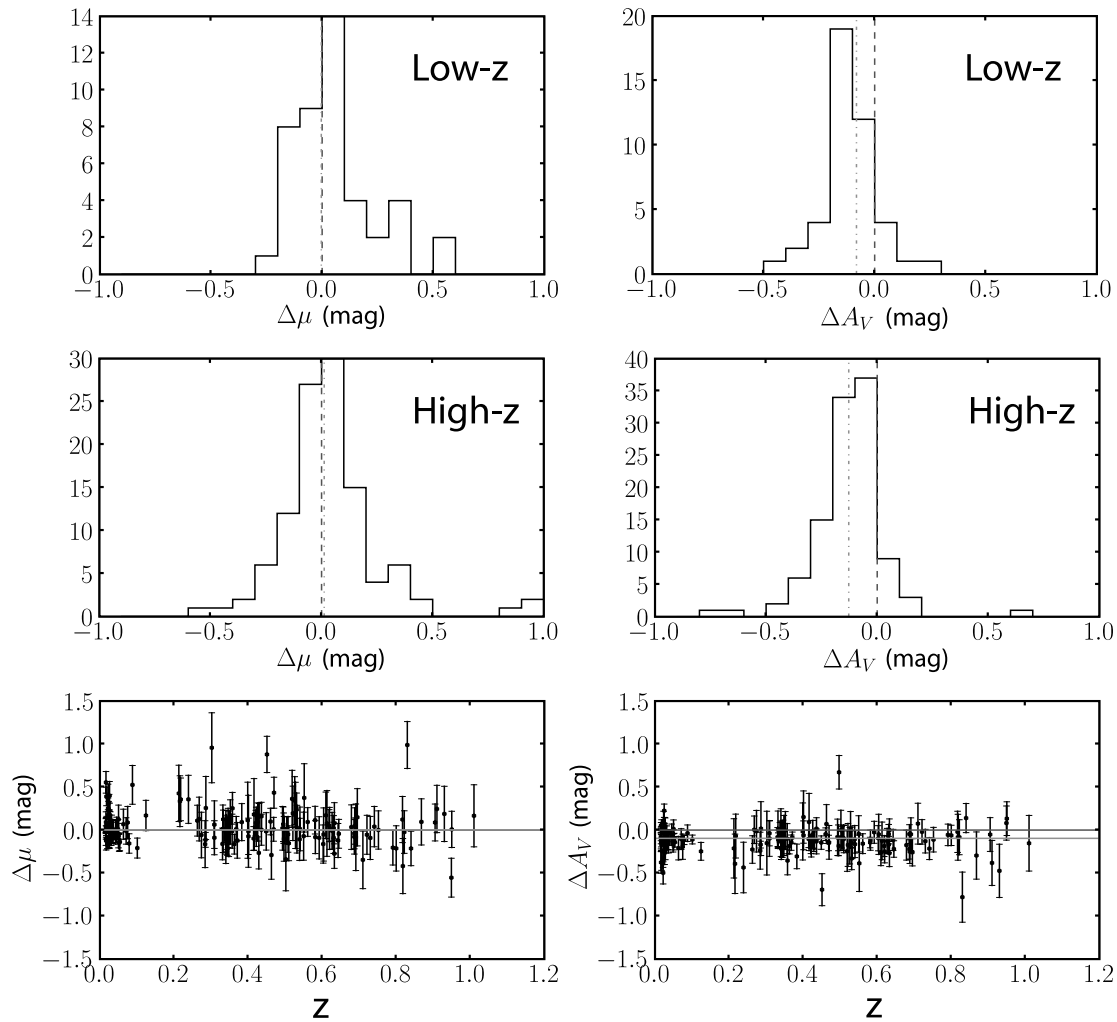
Fig. 5.—Distance modulus and $A_V$ as a function of redshift for MLCS2k2 glosz minus the SALT distance modulus and $\beta \times$ color ($\beta = 1.57$) for the ESSENCE, SNLS, and nearby data sets. High $z$ refers to SNe Ia with $z \geq 0.15$, low $z$ to $z < 0.15$. The dot-dashed line shows the weighted average of the difference for each quantity, while the dashed line shows the line of zero difference. While the luminosity distances are offset between the two fitters, this is mainly due to a slightly different definition of the $\mathcal{M}$ parameter that defines the absolute luminosity of an SN Ia and the Hubble constant. The relative average difference between low redshift and high redshift is $-0.0023$ mag. This agreement translates to a similar agreement in the cosmological parameters obtained with each approach (see Figs. 10 and 11). [*See the electronic edition of the Journal for a color version of this figure.*]

window functions in $A_V$ and $\Delta$. The simulations using the glosz prior provide a median $\Delta\mu$ within 0.03 mag for all redshifts less than 0.7, which we judge to be satisfactory performance. The glosz prior corrects for selection biases that have a significant impact on recovering the true distance moduli at faint magnitudes and high redshift. The need for the glosz prior underscores the importance of understanding selection bias, dust extinction priors, and light-curve width distributions in determining distances at the few percent level in supernova surveys.

## 2.4. *Comparison of MLCS2k2 and SALT Luminosity Distance Fitters*

The release of the source code to the SALT fitter (Guy et al. 2005) makes a modern SN Ia light-curve fitter fully accessible and available to the community. This public release of SALT allows us to compare the results of our MLCS2k2 distance fitter (presented in Table 4) with the SALT fitter used in the SNLS first-results paper (A06). We present the results of SALT fits to our nearby and ESSENCE samples in Table 5. To compute the distance moduli we quote in that table, we assume the $\alpha = 1.52$, $\beta = 1.57$ values from A06.

To calibrate the additional dispersion to add to the distance moduli of MLCS2k2 and SALT, we fitted a $\Lambda$CDM model to the nearby sample alone and derived the additional $\sigma_{add}$ to add in quadrature to recover $\chi^2$/dof of 1 for the nearby sample. This $\sigma_{add}$ is related to the intrinsic dispersion of the absolute luminosity of SNe Ia but is not precisely the same both because the light-curve fitters include varying degrees of model uncertainty and because the light curves of the SNe Ia are subject to photometric uncertainty. We find $\sigma_{add} = 0.10$ mag for MLCS2k2 with the glosz prior and $\sigma_{add} = 0.13$ mag for SALT. These values should be added to the $\sigma_\mu$ uncertainties given in Tables 4 and 5. Figure 5 visually demonstrates that the relative luminosity distances using the SALT light-curve fitter agree, within uncertainties, with the MLCS2k2 distances when the latter are fitted using the glosz $A_V$ prior.

## 2.5. *Testing the Recovery of Cosmological Models Using Simulations of the ESSENCE Data Set*

In order to assess our ability to recover unbiased estimates of the cosmological parameters and the accuracy of our uncertainties, we have carried out a set of Monte Carlo simulations of our
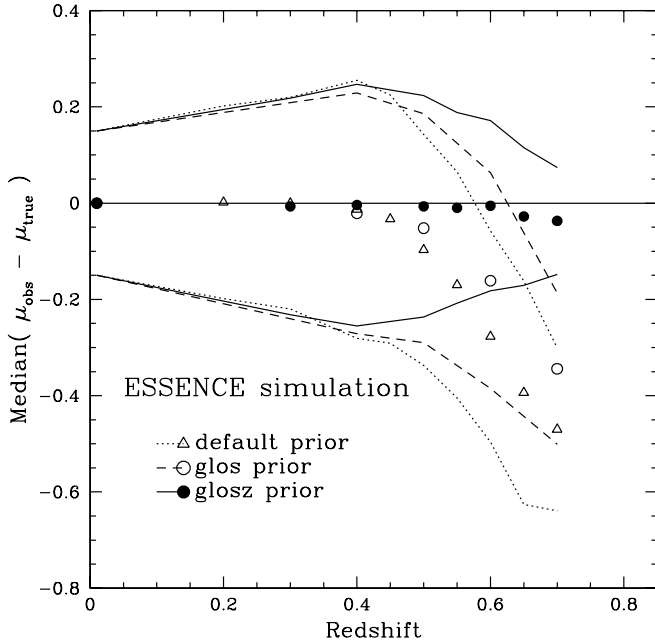
FIG. 6.—Median of the distance modulus error as a function of redshift for the simulated data sets. The points show the median value of the difference between the input $\mu_{\mathrm{true}}$ and recovered $\mu_{\mathrm{obs}}$ of about 1000 simulated supernovae at each redshift. The lines indicate the rms spread of the recovered distance modulus.

data set. We generated 5000 instances of an SN Ia sample designed to be statistically similar to the actual ESSENCE plus nearby sample after application of the quality cuts in Table 1 (in terms of redshift distribution, peculiar velocities, distance modulus errors, etc.) around a fiducial cosmology (flat: $\Omega_M = 0.3$, $\Omega_\Lambda = 0.7$). We then fitted each of these samples to recover ($\Omega_M$, $w$) in a flat universe in combination with the baryon
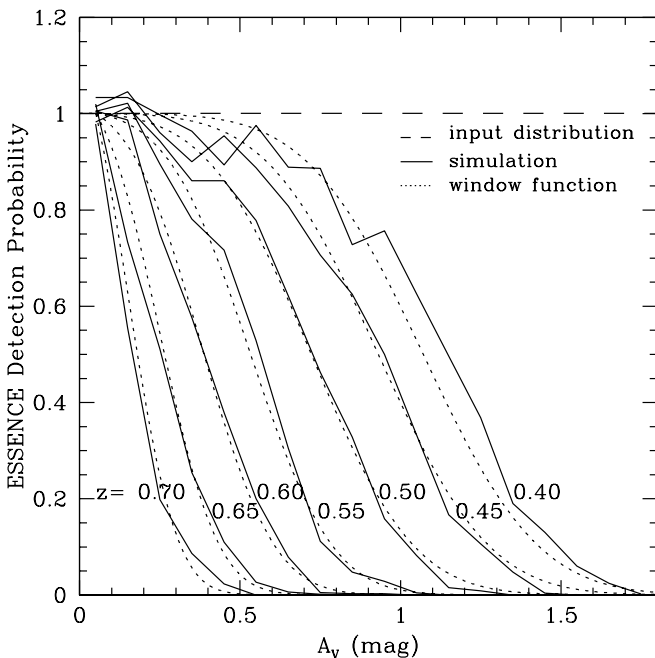


FIG. 7.—Recovered distribution of visual extinctions for simulated supernovae in the ESSENCE sample if the input distribution were uniform in $A_V$ out to large extinctions. The curves are fitted to determine the parameters of the window function (see Table 3), which is then used to modify the glos prior as a function of redshift into the glosz prior. We estimate the SNLS selection function as extending +0.2 in redshift deeper than the ESSENCE selection function.

TABLE 3
"glosz" WINDOW FUNCTION PARAMETERS

| $z$ | $A_{1/2}$ | $\sigma_A$ | $\Delta_{1/2}$ | $\sigma_\Delta$ |
|---|---|---|---|---|
| 0.35 | 1.35 | 2.2 | 0.93 | 2.4 |
| 0.40 | 1.05 | 2.5 | 0.75 | 2.4 |
| 0.45 | 0.88 | 2.6 | 0.60 | 2.6 |
| 0.50 | 0.67 | 2.8 | 0.43 | 2.6 |
| 0.55 | 0.48 | 3.5 | 0.29 | 2.7 |
| 0.60 | 0.33 | 4.0 | 0.17 | 2.8 |
| 0.65 | 0.20 | 5.0 | 0.05 | 3.0 |
| 0.70 | 0.10 | 6.0 | −0.09 | 3.3 |
| 0.75 | 0.05 | 7.5 | −0.25 | 3.3 |

acoustic oscillation (BAO) constraint (Eisenstein et al. 2005). To handle the latter, we shifted the results from this paper to our fiducial cosmology and randomly varied its value around that point using provided uncertainties. We then compared the mean recovered cosmological parameters with the input values and found that they are biased at less than the 1% level. Furthermore, we find that the error estimates on the cosmological parameters are slightly overconservative at about the 0.5% level. Hence, our methodology is sufficiently accurate for our requirements.

## 3. POTENTIAL SOURCES OF SYSTEMATIC ERROR

Here we identify and assess sources of systematic error that could afflict our measurements. These can be divided into two groups. Certain sources of systematic error may introduce perturbations either to individual photometric data points or to the distances or redshifts estimated to the SNe Ia. Others affect the data in a more or less random fashion and produce excess *scatter* in the Hubble diagram. Errors that are uncorrelated with either distance or redshift will not bias the cosmological result. These sources of photometric error are detailed by Miknaitis et al. (2007); we summarize those results here in Table 6. We add these effects in quadrature to the statistical uncertainties given by the luminosity distance fitting codes for each SN Ia distance measurement: $\sigma_\mu^{\mathrm{phot\ scatter}} = 0.026$ mag.

In § 2 we discussed our testing of the MLCS2k2 fitter on simulated data sets that replicate the data quality of the ESSENCE and nearby SNe Ia. We explore the issue of host galaxy extinction further in §§ 3.3 and 3.4. The interaction of Malmquist bias and selection effects with the extinction and color distribution of SNe Ia is discussed in § 3.5.

Any noncosmological difference in measurements of nearby and distant SNe Ia has the potential to perturb our measurement of $w$. Table 7 lists potential systematic effects of this sort. We present both our estimate of the sensitivity ($dw/dx$) of the equation-of-state parameter to each potential systematic effect and our best estimate of the potential size of the perturbation, $\Delta x$. The upper bound on the bias introduced in $w$ is then $\Delta w = (dw/dx)\Delta x$. Miknaitis et al. (2007) discuss the systematic uncertainties on $\mu$, which we convert here to systematic uncertainties on $w$, due to photometric errors from astrometric uncertainty on faint objects ($\Delta w = 0.005$), potential biases from the difference imaging ($\Delta w = 0.001$), and linearity of the MOSAIC II CCD ($\Delta w = 0.005$). None of these contributed noticeably to the systematic uncertainty in our measurement of $w$. The rest of this section describes how we appraised our additional potential sources of systematic uncertainty.

The conclusion of this section is that our current overall estimate for the 1 $\sigma$ equivalent systematic uncertainty in a

TABLE 4
MLCS2k2 "glosz" Luminosity Distances of All SNe Ia

| Name | $z$ | $\sigma_z$[a] | $\mu$ (mag) | $\sigma_\mu$[b] (mag) | $A_V$ (mag) | $\sigma_{A_V}$ (mag) | $\Delta$ | $\sigma_\Delta$ | $T_{max}$ (MJD) | $\sigma_{T_{max}}$ (MJD) | $\chi^2$/dof | dof | $T_{first}$ (days) | $T_{last}$ (days) | Failed |
|---|---|---|---|---|---|---|---|---|---|---|---|---|---|---|---|
| b010............ | 0.5910 | 0.007 | 42.984 | 0.223 | 0.104 | 0.094 | −0.166 | 0.182 | 52592.80 | 2.69 | 1.01 | 3 | 0.22 | 19.70 | Y |
| b013............ | 0.4260 | 0.004 | 41.976 | 0.228 | 0.170 | 0.149 | +0.034 | 0.141 | 52586.33 | 1.51 | 0.22 | 12 | −2.21 | 35.64 | N |
| b016............ | 0.3290 | 0.003 | 41.349 | 0.423 | 0.359 | 0.275 | +0.190 | 0.384 | 52587.76 | 2.29 | 3.31 | 1 | −0.56 | 16.76 | Y |
| b020............ | 0.4250 | 0.003 | 41.766 | 0.384 | 0.202 | 0.204 | +0.059 | 0.323 | 52599.88 | 0.90 | . . . | 0 | −8.94 | 7.21 | Y |
| d033............ | 0.5310 | 0.008 | 42.960 | 0.170 | 0.085 | 0.091 | −0.322 | 0.109 | 52934.26 | 1.87 | 0.98 | 5 | −2.12 | 23.41 | N |

Notes.—The relative luminosity distance moduli and extinctions as determined by MLCS2k2 of the full ESSENCE SNe Ia and nearby sample using the "glosz" prior (Hatano et al. 1998; Commins 2004; Riello & Patat 2005) described in § 2. SN Ia fits marked as "Failed" did not pass the MLCS2k2 quality cuts given in Table 1. See Table 1 and § 2 for further discussion of the quality cuts applied here. Redshifts of SNe Ia come from SNID fits (Miknaitis et al. 2007; Blondin & Tonry 2007).
[a] We add a 400 km s$^{-1}$ peculiar velocity dispersion in quadrature to these redshift uncertainties for our cosmological fits.
[b] An "intrinsic" dispersion of $\sigma_\mu = 0.10$ mag has been added in quadrature to the values output by MLCS2k2 (Jha et al. 2006a) to fully account for the intrinsic dispersion of SNe Ia.

static equation-of-state parameter is $\Delta w = 0.13$ for our glosz analysis.

### 3.1. Photometric Zero Points

Supernova cosmology fundamentally depends on the ability to accurately measure fluxes of objects over a range in redshift. Errors in photometric calibration translate to errors in cosmology in two basic ways, as follows.

Nearby objects at redshifts <0.1 play a crucial role in establishing a comparison reference for cosmological measurements. ESSENCE is inefficient at finding and observing low-redshift objects with the same telescope and detector system, so we use photometry of low-redshift SNe Ia in the literature from our own work and that of others (for the full list see Jha et al. 2007). Using these external SNe Ia requires understanding the photometric calibration of our high-redshift sample relative to this low-redshift sample. Every supernova cosmology result to date has made use of more or less the same low-redshift photometry, so any inaccuracies in the nearby sample are a source of common systematic error for all SN Ia cosmology experiments. Calibration of photometry at the ∼1% level required to make precise inferences about the nature of dark energy is notoriously difficult (Stubbs & Tonry 2006).

Photometric miscalibration can result in a second, more insidious systematic error if there is an error in the relative flux scaling between the broadband passbands. This offset would distort the observed colors for the entire sample. Since these colors are used to infer the extinction, even small color errors result in significant biases in the measured distances. After all,

the inferred host galaxy extinction, $A_V$, is related to the measured color excess, $E(B − V)$, by $A_V \approx 3.1E(B − V)$ (for Milky Way–like dust). A color error in rest-frame $B − V$ (observer-frame $R − I$ for ESSENCE) of 0.01 mag can result in 0.03 mag error in extinction, an inaccuracy that would lead directly to a 3% error in the distance modulus, or a 1.5% error in the distance. We currently estimate our color zero-point uncertainty to be 0.02 mag and our absolute zero-point (relative to the nearby SNe Ia) uncertainty to be 0.02 mag. These respectively translate to 0.04 and 0.02 shifts in $w$ (see Table 7).

Miknaitis et al. (2007) describe the calibration program we undertook to measure the transmission of the CTIO 4 m MOSAIC II system with the $R$ and $I$ filters of the ESSENCE survey. The calibration of the ESSENCE survey fields will be further improved by an intensive calibration program we have undertaken on the CTIO 4 m telescope. The improved calibration of Stripe 82 of the SDSS Southern Survey by the SDSS-II project, which overlaps 25% of our ESSENCE fields, will provide an important cross-check for the spatial homogeneity of our photometric system. We aim to achieve 1% photometric calibration of our CTIO 4 m MOSAIC II *BVRI* natural system.

Here we use MLCS2k2 v004 with the Bohlin & Gilliland (2004) values for the magnitudes of Vega, i.e., `alpha_lyr_stis_002.fits` with $R_{Vega} = 0.033$ mag. This value for $R_{Vega}$ comes from Bessell et al. (1998) but has been shifted down by 0.004 mag as Bohlin & Gilliland (2004) suggest (from their $V_{Vega} = 0.026$ mag compared to $V_{Vega} = 0.030$ mag from Bessell et al. 1998).

TABLE 5
SALT Luminosity Distances of All SNe Ia

| Name | $z$ | $\sigma_z$[a] | $\mu$ (mag) | $\sigma_\mu$[b] (mag) | Color | $\sigma_{color}$ | Stretch | $\sigma_{stretch}$ | $T_{max}$ (MJD) | $\sigma_{T_{max}}$ (MJD) | $\chi^2$/dof | dof | Rise | Tail | Failed |
|---|---|---|---|---|---|---|---|---|---|---|---|---|---|---|---|
| b010................. | 0.5910 | 0.007 | 43.524 | 0.274 | −0.127 | 0.086 | 1.232 | 0.141 | 52589.42 | 4.98 | 0.99 | 15 | 0 | 19 | Y |
| b013................. | 0.4260 | 0.004 | 42.144 | 0.155 | +0.077 | 0.039 | 1.012 | 0.050 | 52586.02 | 0.94 | 0.71 | 13 | 2 | 15 | N |
| b016................. | 0.3290 | 0.003 | 41.876 | 0.213 | +0.246 | 0.102 | 1.121 | 0.002 | 52579.73 | 0.05 | 0.73 | 6 | 0 | 10 | N |
| b020................. | 0.4250 | 0.003 | 41.696 | 0.341 | +0.068 | 0.176 | 0.840 | 0.111 | 52599.81 | 1.07 | . . . | 0 | 1 | 3 | Y |
| d033................. | 0.5310 | 0.008 | 43.271 | 0.188 | −0.156 | 0.059 | 1.150 | 0.088 | 52932.50 | 1.70 | 1.74 | 17 | 2 | 19 | N |

Notes.—The relative luminosity distance moduli and colors as determined by SALT of the full SNLS, ESSENCE, and nearby SN Ia sample. SN Ia fits marked as "Failed" did not pass the SALT quality cuts given in Table 2. The SALT fitter quotes minimum $\chi^2$ values for the light-curve fit parameters rather than estimated mean estimated parameters. See Table 2 for the quality cuts applied here.
[a] We add a 400 km s$^{-1}$ peculiar velocity dispersion in quadrature to these redshift uncertainties for our cosmological fits.
[b] An "intrinsic" dispersion of $\sigma_\mu = 0.13$ mag has been added in quadrature to the values output by SALT (Guy et al. 2005) to fully account for the intrinsic dispersion of SNe Ia.

TABLE 6
SOURCES OF INCREASED $\mu$ DISPERSION

| Source | $\sigma_\mu$ |
|---|---|
| Flat-fielding | 0.01 |
| Focal plane PSF | 0.02 |
| Field-field zero point | 0.01 |
| Image subtraction | 0.01 |
| Subtotal (quadrature sum) | 0.026 |
| Gravitational lensing | 0.04 |
| Total (quadrature sum) | 0.05 |

NOTE.—The photometric and astrophysical uncertainties that add increased scatter, but no bias, to the measured SN Ia distance moduli, $\mu$.

### 3.2. *K-Corrections and Bandpass Uncertainty*

Uncertainty in the transmission function, typically called the bandpass, of the optical path of the telescope+detector is an important and potentially systematic effect. In this context, bandpass refers to the wavelength-dependent throughput of the entire optical path, including atmospheric transmission, mirror reflectivity, filter function, and CCD response. Since an error in the assumed bandpasses translates into a redshift-dependent error in the supernova flux, it is important to account for possible errors in the bandpass estimates.

The *relative* error due to bandpass miscalibration is small for objects with similar spectra, such as SNe Ia. Bandpass shape errors are largely accounted for by the filter zero-point calibration, with residual errors corresponding to the difference between the spectral energy distribution of the objects of interest and those of the calibration sources. In the case of SN Ia observations, any residual zero-point error is absorbed when we marginalize over the "nuisance parameter," $\mathcal{M} = M_B - 5\log_{10}(H_0) + 25$ (Kim et al. 2004). This relative comparison results in a very small systematic error in the cosmological

parameters from a global calibration error across bandpasses. Moreover, variations in atmospheric transmission are expected to contribute only random uncertainty.

However, the bandpass uncertainty becomes important when we compare SNe Ia at different redshifts for which the bandpass samples different spectral regions. In order to compare SNe Ia at multiple redshifts, we need to perform a *K*-correction (Leibundgut 1990; Hamuy et al. 1993; Kim et al. 1996; Nugent et al. 2002); that is, we assume a spectral distribution for the supernova and convert the observed magnitude to what it would have been had the supernova been at another redshift. This process involves performing synthetic photometry of the assumed spectral distribution over the assumed bandpass. We address the issue of systematics arising from errors in the assumed spectral distribution in § 3.6. Here we address systematics arising from errors in our determination of the CTIO 4 m MOSAIC II *R* and *I* bandpass functions. Systematic effects on supernova cosmology that result from bandpass uncertainties are discussed more thoroughly by Davis et al. (2006).

Calculating the effect of bandpass uncertainty is fairly difficult because of the arbitrary nature of the shape changes that might affect the bandpass. However, we can make several general calculations. As a first step, we take standard bandpasses and add white noise to represent a miscalibrated filter. White noise contributes power on all scales, so this approach adds small-scale discrepancies as well as large-scale warps or shifts in the filter. By averaging over many such miscalibrated filters, we can estimate the effect of filter miscalibration. Figure 16 of Davis et al. (2006) shows photometric error as a function of noise amplitude. A noise amplitude of 0.02 produces a typical deviation of 2% from the nominal filter shape at any wavelength. Calibrating the bandpass to better than 3% allows us to keep the *K*-correction error introduced from a mismeasurement of our effective bandpass to less than 0.005 mag (0.5% in flux) and a systematic uncertainty of $\Delta w = 0.005$.

TABLE 7
POTENTIAL SOURCES OF SYSTEMATIC ERROR ON THE MEASUREMENT OF $w$

| Source | $dw/dx$ | $\Delta x$ | $\Delta_w$ | Notes |
|---|---|---|---|---|
| Photometric errors from astrometric uncertainties of faint objects | 1/mag | 0.005 mag | 0.005 | |
| Bias in differential image photometry | 0.5/mag | 0.002 mag | 0.001 | |
| CCD linearity | 1/mag | 0.005 mag | 0.005 | |
| Photometric zero-point differences in $R$, $I$ | 2/mag | 0.02 mag | 0.04 | |
| Zero-point offset between low and high $z$ | 1/mag | 0.02 mag | 0.02 | |
| *K*-corrections | 0.5/mag | 0.01 mag | 0.005 | |
| Filter passband structure | 0/mag | 0.001 mag | 0 | |
| Galactic extinction | 1/mag | 0.01 mag | 0.01 | |
| Host galaxy $R_V$ | 0.02/$R_V$ | 0.5 | 0.01 | "glosz" |
| Host galaxy extinction treatment | 0.08 | Prior choice | 0.08 | Different priors |
| Intrinsic color of SNe Ia | 3/mag | 0.02 mag | 0.06 | Interacts strongly with prior |
| Malmquist bias/selection effects | 0.7/mag | 0.03 mag | 0.02 | "glosz" |
| SN Ia evolution | 1/mag | 0.02 mag | 0.02 | |
| Hubble bubble | 3/$\delta H_{effective}$ | 0.02 | 0.06 | |
| Gravitational lensing | 1/$\sqrt{N}$/mag | 0.01 mag | <0.001 | Holz & Linder (2005) |
| Gray dust | 1/mag | 0.01 mag | 0.01 | |
| Subtotal without extinction+color | ... | ... | 0.082 | |
| Total | ... | ... | 0.13 | |
| Joint ESSENCE+SNLS comparison | ... | ... | 0.02 | Photometric system |
| Joint ESSENCE+SNLS total | ... | ... | 0.13 | |

NOTES.—The systematic error table for this first ESSENCE cosmological analysis. The issue of treatment of $A_V$ and color distribution is clearly the dominant systematic effect and will need to be seriously addressed to reduce our systematic errors to our target of 5%.

### 3.3. *Extinction*

The most significant cause of variation in the apparent luminosity of SNe Ia is the extinction experienced by the light from the SN Ia due to scattering and absorption by dust in the host galaxy.

Dust introduces a wavelength-dependent diminution of a supernova's light. In the case of Milky Way dust, we correct for its effects by using tabulated values as a function of Galactic longitude and latitude measured by other means (see SFD98), being sure in our MLCS2k2 fits to properly account for its uncertainty and correlation across all observations. For dust in the supernova's host galaxy, we infer the extinction from the reddening of each supernova's light curve.

However, the slope of differential reddening, characterized in the Cardelli et al. (1989) extinction model by the parameter $R_V$, may vary. The nominal value of $R_V$ for the Milky Way is 3.1, but different lines of sight within our Galaxy have values of $R_V$ that vary from 2.1 to 5.1. Studies of $R_V$ in other galaxies have been more limited because we lack sources of known color and luminosity with which to probe the dust.

Because we use the supernova rest-frame $B - V$ color to determine the reddening of each SN Ia, and the distance modulus to a supernova is corrected by a value approximately 3 times the inferred reddening, extinction correction magnifies any source of systematic error in a supernova's observed effective color. Systematic color errors can result from photometry errors, redshift-dependent $K$-correction errors, and evolution in the colors of supernovae.

Using the IR emission maps of the Galaxy from the all-sky *COBE* DIRBE and *IRAS* ISSA maps, SFD98 have estimated the dust column density around the sky, which can then be translated to a color excess. This analysis has largely superseded the work of Burstein & Heiles (1978), who used radio H I measurements and a relationship between gas and extinction to estimate the color excess across the sky. Burstein (2003) has reanalyzed the IR and H I measurements and finds that Milky Way extinctions are more precisely derived using the IR method. However, Burstein (2003) still finds a discrepant value for extinction at the poles, with SFD98 providing extinctions that are $E(B - V) = 0.02$ mag higher than what the H I measurements indicate. Burstein (2003) suggests as a possible explanation for the discrepancy that SFD98 may predict too large an extinction in areas with high gas-to-dust ratios. Finkbeiner et al. (1999) precisely estimated their sensitivities to these systematics and concluded that they had controlled them to 0.01 mag. The ESSENCE program targets fields at high Galactic latitude to minimize Galactic extinction. Although nearby and distant SNe Ia are both affected by the assumed Milky Way extinction, the nearby objects are observed in $B - V$, whereas the $z \approx 0.5$ objects are observed in $R - I$. An $E(B - V) = 0.02$ difference in extinction at the pole leads to approximately a 0.02 mag difference in the relative distances between $z = 0$ and $z = 0.5$ objects, assuming a Galactic reddening law, host galaxy corrections based on rest-frame $B - V$ color, and distances based on $V$. For this analysis, we use the SFD98 extinction map values with an uncertainty of 16% for each individual SN Ia but assume an additional 0.01 mag of systematic uncertainty in our distance moduli to account for the known source of extinction uncertainty at the pole.

In most supernova work we assume that the Galactic reddening law (Cardelli et al. 1989) applies to external galaxies ($R_V = 3.1$), but studies of individual SNe Ia have found a range of values extending to much smaller values of $R_V$ (Riess et al. 1996; Tripp 1998; Phillips et al. 1999; Krisciunas et al. 2000;

TABLE 8
EFFECT OF DIFFERENT FIXED $R_V$ ON $w$ FOR THE TWO DIFFERENT
$A_V$ PRIORS CONSIDERED IN OUR MLCS2k2 ANALYSIS
OF THE ESSENCE+NEARBY SAMPLE

| $A_V$ Prior | $R_V$ Value | $w$ | $w - w_{R_V=3.1}$ for Given Prior |
|---|---|---|---|
| glosz ................... | 2.1 | $-0.986^{+0.116}_{-0.114}$ | +0.061 |
| | 3.1 | $-1.047^{+0.125}_{-0.124}$ | ... |
| | 4.1 | $-1.073^{+0.121}_{-0.120}$ | −0.026 |
| glos ..................... | 2.1 | $-0.932^{+0.116}_{-0.114}$ | +0.025 |
| | 3.1 | $-0.957^{+0.127}_{-0.124}$ | ... |
| | 4.1 | $-1.039^{+0.134}_{-0.131}$ | −0.082 |
| Exponential ........ | 2.1 | $-0.855^{+0.126}_{-0.122}$ | +0.027 |
| | 3.1 | $-0.882^{+0.134}_{-0.130}$ | ... |
| | 4.1 | $-0.808^{+0.147}_{-0.141}$ | +0.074 |

NOTE.—Systematic effect of choosing different fixed $R_V$ values for the different $A_V$ priors discussed here for MLCS2k2.

Wang et al. 2003; Altavilla et al. 2004; Reindl et al. 2005; Elias-Rosa et al. 2005). These measurements are dominated by objects with large extinction values, where a significant measurement can be made of the extinction law (lessening the effects of intrinsic color scatter and systematic color variations with luminosity), and it is possible that $R_V$ is correlated with total extinction (Jha et al. 2007). In principle, with photometry in three or more passbands, it is possible to fit for $R_V$, but in practice, at $z > 0.2$, there are only a few SNe Ia in the literature with the requisite high-precision photometry extending from the rest-frame UV to the near-IR. The systematic error on our measurement of $D_L$ caused by assuming a particular value of $R_V$ depends on the average extinction as a function of redshift, assuming that $R_V$ is constant with $z$, except for a small correction caused by the rest-frame effective bandpass of our filters drifting away from the low-$z$ values, depending on the precise redshift of each object. To quantify this effect, we fit our complete distance set with three different values of $R_V$: 2.1, 3.1, and 4.1.

### 3.4. *Color and Extinction Distributions and Priors*

To evaluate the systematic effects produced by various prior assumptions about extinction, we have fitted the entire data set with a variety of plausible priors: the "exponential" prior of Jha et al. (2007), a flat prior from $-\infty$ to $+\infty$ (the flatnegav prior), and an exponential prior with an added Gaussian around zero that is based on models of the dust distribution in galaxies (glos and the redshift-dependent glosz). These results are presented in § 4 and form the basis for Table 8.

To separate the effects of color and extinction, Jha et al. (2007) noted that the distribution of color excess in their nearby sample was consistent with a Gaussian distribution of $\sigma = 0.2$ mag convolved with a one-sided exponential, $\exp(-A_V/\tau)$, where $\tau = 0.46$ mag. As discussed in § 2.2, the glosz prior we adopt here is derived from models of line-of-sight dust distributions in galaxies. It has more parameters than the simple exponential model of Jha et al. (2007), but we believe that these additional parameters are well motivated.

The power of MLCS2k2 to distinguish between color and extinction lies in the ability to treat the two phenomena independently. A06 use SALT and make the assumption that the color+extinction distribution is the same in the nearby and in the high-redshift samples; the separation of the $A_V$ component in the MLCS2k2 model allows us to model our expected distribution of $A_V$ based on both models of dust in galaxies and selection effects of the ESSENCE survey. This separation allows

us to take the nominal glos model and create the glosz prior that combines the distribution of dust in galaxies with the redshift-dependent selection effects.

The difference in the mean estimated parameter for a constant $w$ is given in Table 8 for the different MLCS2k2 $A_V$ priors discussed above. For the main MLCS2k2 glosz analysis we present here, we find a slope of $\Delta w/\Delta R_V = 0.02$ in the dependence of $w$ on the assumed value of $R_V$. The effect on $w$ of varying $R_V$ is substantially greater for the less restrictive $A_V$ priors because the covariance between $A_V$ and $\mu$ is substantially greater for these priors. A reasonable variation of 0.5 in the value for $R_V$ contributes a systematic uncertainty of $\Delta w = 0.01$.

Differences in the inferred value of $w$ for various assumed absorption priors show that this is a significant systematic effect. The maximum difference between two priors, exponential and glosz, for the nominal $R_V = 3.1$ case is $\Delta w = 0.165$. While we have conducted careful simulations to determine the most appropriate prior for our sample (see § 2.3) and it is clear that the exponential prior is not appropriate for this analysis, we nonetheless take half of the difference between the two as representative of our systematic uncertainty, $\Delta_w^{\mathrm{prior}} = 0.08$, due to the choice of prior. The residual 0.02 mag shift of the simulations with the glosz prior shown in Figure 7 for $z \approx 0.65$ results in a very small shift in $\Delta w$ of only 0.001.

Because we use a one-sided $A_V$ prior, we are sensitive to our ability to determine the intrinsic color distribution of SNe Ia. We estimate the contribution of our uncertainty in the intrinsic SN Ia color distribution to our systematic error budget at $\Delta w = 0.06$.

We have not undertaken a similar analysis with the SALT fitter, but the underlying assumption that the color-extinction-luminosity relationship for SNe Ia is constant with redshift is subject to uncertainties analogous to those considered here in the context of the MLCS2k2 $A_V$ prior. The issue of color and extinction distributions clearly needs to be addressed for substantial further progress to be made in the field of supernova cosmology.

### 3.5. *Malmquist Bias and Other Selection Effects*

As with all magnitude-limited surveys, at the faint limits of the survey we are more likely to observe objects drawn from the bright end of the SN Ia luminosity distribution. This Malmquist bias is particularly dangerous for inferences about cosmology based on supernova observations. However, it is not necessarily troubling that we may observe more luminous, broad events at high redshift, as long as the known empirical luminosity-width relation is valid at those redshifts. Rather, the concern for cosmological measurements is that at high redshift, we may preferentially find SNe Ia that are bright *for their light-curve shape*. A second and more subtle concern is that at higher redshifts we are also less likely to detect SNe Ia whose light suffers significant absorption due to dust in their host galaxies.

We have modeled both of these effects (see §§ 2.3 and 3.3) and have controlled for their impact. Our current limits on systematics due to uncontrolled selection effects are $\Delta_w^{\mathrm{selection}} = 0.02$. A thorough study of the efficiency of the ESSENCE survey will be presented by G. Pignata et al. (2007, in preparation). We aim for this future work to allow us to reduce this contribution to our systematic error to no more than 1%.

### 3.6. *Type Ia Supernova Evolution*

A persistent concern for any standard candle cosmology is the possibility that the distant candles may differ slightly from their low-redshift counterparts. In a recent paper (Blondin et al. 2006) we compare the spectra of the high-redshift SNe Ia in this sample with those of low-redshift SNe Ia and demonstrate that there is no evidence for any systematic difference in their properties. This conclusion is based on line profile morphology and measurements of the phase evolution of the velocity location of maximum absorption and peak emission.

These results confirm a number of other studies of distant SNe Ia (e.g., Coil et al. 2000; Sullivan et al. 2003; Lidman 2004) that all suggest that, to the accuracy of current observations, the high- and low-redshift supernova populations are indistinguishable. Recently, Hook et al. (2005) used spectral dating, spectral time sequences, and measurements of expansion velocities to compare distant and nearby SNe Ia; they also find no evidence for evolution in SN Ia properties up to $z \approx 0.8$.

Although we are confident that the subtypes of distant SNe Ia are well represented by the subtypes seen nearby, we cannot rule out a subtle shift in the population demographics that may yet bias the estimates of cosmological parameters. This potential bias is of particular concern for future experiments that plan to measure the equation-of-state parameter, $w$, with an accuracy of a few percent. There is now evidence that SN Ia properties are correlated with host galaxy morphology. Hamuy et al. (1996) and Riess et al. (1999) show that the most luminous SNe Ia occur only in galaxies with ongoing star formation. Sullivan et al. (2006b) use SNLS SNe Ia to confirm these findings for SNe Ia at high redshift. They similarly find one population of generally slower declining SNe Ia in galaxies with recent star formation and another of generally faster declining SNe Ia in galaxies with no ongoing star formation. However, no residual correlation after light-curve shape correction is observed in any of these studies.

This correlation between SN Ia light-curve width and galaxy environment implies that improved understanding of host galaxies may be important for improving the use of SNe Ia as standard candles. On the other hand, the confirmation of the same correlations at high and low redshifts is a reassurance that the fundamental mechanisms that generate SNe Ia remain the same. Because the galactic demographics over the redshift range of interest change less than current variations in the stellar populations of low-redshift SN Ia host galaxies, we remain confident that our one-parameter correction for supernova luminosity adequately corrects any shift in the average luminosity of SNe Ia to the same precision as in the nearby universe, $\sigma_\mu < 0.02$ mag. We thus estimate a systematic uncertainty from possible SN Ia evolution on our measurement of $w$ of $\Delta w = 0.02$.

One way to verify this confidence is to search for additional parameters that allow tighter luminosity groupings of the low-redshift population. In a first, reassuring step, Hubble diagrams for subsets of SNe Ia based on host galaxy type separately confirm the accelerating expansion of the universe (Sullivan et al. 2003).

### 3.7. *Hubble Bubble and Local Large-Scale Structure*

The local large-scale structure and associated correlated flows of the universe should not yet present a significant contribution to the systematic error budget of the current survey (Hui & Greene 2006; Cooray & Caldwell 2006). However, at the lowest multipoles we are sensitive to local correlated flows, and at the most extreme, our cosmological results would be sensitive to a local velocity monopole or "Hubble bubble." Jha et al. (2007) see such an effect in their analysis of nearby SNe Ia. We use only the subset of SNe Ia from Jha et al. (2007) with $z > 0.015$ and

find that this effect could contribute as much as 0.065 to our systematic error budget in $w$. We will rely on future sets of nearby SNe Ia ($0.01 < z < 0.05$) that are now being acquired at the CfA, by the Carnegie Supernova Program, by the Lick Observatory Supernova Search, and by the Nearby Supernova Factory to reduce this uncertainty below 2% to help achieve the desired systematic uncertainty required for the final ESSENCE analysis.

### 3.8. Gravitational Lensing

Gravitational lensing can increase or decrease the observed flux from a distant object. The expected distribution is asymmetric about the average flux multiplier of unity. Holz & Linder (2005) calculate the effect for SN Ia surveys and determine that any systematic effect from neglecting the asymmetry of the probability distribution function for magnification (as we do here) decreases quickly with the number of SNe Ia per effective bin. Roughly speaking, at $z \approx 0.5$, in a redshift bin width of $\Delta z \approx 0.1$, 10 SNe Ia per bin are sufficient to reduce any systematic effect in luminosity distance to less than 0.3%, which makes no noticeable contribution to our systematic error budget. For the redshifts of interest in the ESSENCE survey, lensing has a more significant effect in the scatter it adds to the observed brightness of SNe Ia. Holz & Linder (2005) calculate a $\sigma_{\rm eff} = 0.04$ mag quadrature increase in the dispersion in distance modulus at $z \approx 0.5$.

We quantitatively explored the possibility that our supernova sample suffers from gravitational lensing by foreground structures, yielding a systematic lensing rms in excess of the amount predicted by Holz & Linder (2005). To do this, we examined the environment around the 43 of our SNe Ia that lie in the footprint of the Sloan Digital Sky Survey Data Release 3 (SDSS DR3; Abazajian et al. 2005). We extracted all SDSS-classified stars and galaxies within $10'$ of each of our supernovae. We restricted our matches to those objects brighter than $r = 21$ mag, where star-galaxy discrimination is known to be effective, with quality flags indicating that the object was measured as a "primary" object, and with data taken during a "good" observation. Next, we derived the cross-correlation coefficient between each supernova's residual from the Hubble diagram in a $\Lambda$CDM universe and the number of stars or galaxies within an aperture of $10'$ radius, similar to the method of Ménard & Dalal (2005). An uncertainty on each value was determined through bootstrap resampling. We found a correlation coefficient of $-0.031 \pm 0.136$ for stars, consistent with zero correlation as expected. Using galaxies, we found a correlation coefficient of $-0.074 \pm 0.144$, also a null result and an indication that our particular sample is not significantly impacted by gravitational lensing. We repeated the above analysis using a smaller aperture of radius $2'$, where the lensing signal is expected to be stronger but there are fewer neighbors to yield the cross-correlation coefficients. The results of this analysis are consistent with the null results from the $10'$ aperture analysis. We therefore conclude that the systematic error from lensing is negligible for this present sample and analysis.

We include the effect of lensing in our analysis by adding a statistical dispersion of $\sigma_\mu^{\rm lensing} = 0.04$ mag to our luminosity distance modulus uncertainty for the ESSENCE and SNLS SNe Ia.

### 3.9. Gray Dust

When the first cosmological results with SNe Ia were announced, that distant SNe Ia were dimmer than they would be in a decelerating universe, Aguirre (1999a, 1999b) suggested various models for intergalactic gray dust that could explain this dimming without producing observable reddening. To explain

SNe Ia becoming consistently dimmer with distance, this dust would need to be distributed throughout intergalactic space beginning at least at $z = 2$ (Goobar et al. 2002). The most naive model of such dust distribution and creation would predict that SNe Ia should continue to get dimmer relative to a flat, $\Omega_M = 1$ cosmology all the way up to at least a redshift of 2. The high-redshift SN Ia work of Riess et al. (2004, 2007) demonstrated that this continued dimming is not what is observed: the apparent magnitudes of SNe Ia become first a little dimmer and then a little brighter with redshift than they would in an empty universe. This is exactly what we expect from an early phase of deceleration followed by a recent phase of acceleration in a mixed, dark matter/dark energy cosmology.

A more complicated model of dust was contrived by Goobar et al. (2002). It involves the creation of intergalactic dust at just the right rate to match the decrease in opacity due to expansion of the universe. This carefully constructed model mimics the signal of an accelerating universe and is difficult to distinguish from a universe that is presently dominated by dark energy. A related model was recently developed by Robaina & Cepa (2007) that ties this form of replenishing gray dust to the star formation rate. However, gray dust models generically lead to different predictions for luminosity distance and angular diameter distance measurements than accelerating universe models (Kunz & Bassett 2004; Bassett & Kunz 2004). Future improved constraints from angular diameter distance measurements as a function of redshift will provide a valuable cross-check on the luminosity distance measurements that currently give the greatest direct kinematic evidence for dark energy. In general, replenishing gray dust models do not have a strong underpinning in the behavior of known dust and represent a form of fine-tuning. In the larger context of converging cosmological evidence, this particular scheme for matching the data seems less plausible than a universe with dark energy.

Physical models of gray dust involve dust grains with a physical size significantly larger than the wavelength of light being absorbed. While these sources will be gray absorbers for the optical rest-frame and redshifted light in question, they will re-emit this same energy as a blackbody at their characteristic temperature. Even cold dust grains that are not visible in the optical or IR will be visible in the far-infrared. The COBE measurements with the FIRAS instrument (Mather et al. 1990, 1993) would be sensitive to this radiation. Aguirre & Haiman (2000) used the FIRAS measurements (Fixsen et al. 1996, 1998) to place limits on intergalactic gray dust. Similar arguments apply to gray dust in our own Milky Way from the observed lack of emission and structure seen in the FIRAS spectrum. It is difficult to conceal sufficient gray dust to affect the SN Ia observations without creating a detectable signal in the FIRAS maps.

Recent observational constraints from non–SN Ia sources have independently placed significant constraints on the amount of intergalactic dust (Petric et al. 2006; Östman et al. 2006). In particular, the observations of Petric et al. (2006) limit intergalactic dust to contributing no more than 1% to potential dimming of light out to a redshift of 0.5, based on upper limits to X-ray scattering by dust along the line of sight to a quasar at $z = 4.3$.

### 4. COSMOLOGICAL RESULTS FROM THE ESSENCE FOUR-YEAR DATA

The ESSENCE SNe Ia allow us to test the hypothesis of a $\Lambda$CDM concordance model and constrain flat, constant-$w$ models of the universe. We use our MLCS2k2 light-curve fitting technique to measure luminosity distances to nearby and ESSENCE

SNe Ia (Table 4). We then fit cosmological models to constrain the properties of the dark energy, and we compare the results we obtain using MLCS2k2 with those obtained using the SALT light-curve fitter (Guy et al. 2005). The SALT fitter was used to fit the nearby light curves, our ESSENCE light curves, and the SNLS light curves (see footnote 22). To verify that we were making appropriate use of the fitter, we fitted the nearby and SNLS light curves with SALT, taking the same $\alpha = 1.52$ and $\beta = 1.57$ width and color parameters used by A06. We recovered the $w$ result of A06 to within 0.01 in best-fit constant $w$ in a model with a flat universe using the cosmology fitter that we employ here.[23]

This cosmology fitter uses a grid-based approach and calculates the relative likelihood at each grid coordinate in the multidimensional parameter space. Estimates for individual cosmological parameters are calculated by marginalizing the distribution over all other fit parameters. The probability-weighted mean is taken as the central quoted value, and the 1 $\sigma$ uncertainty limits are computed by finding the 34.13% integrated probability to either side of this central value. We have compiled our light curves of nearby SNe Ia from the literature independently of the SNLS analysis and used slightly different quality cuts, so it is quite encouraging that we can replicate these results. Table 5 gives the SALT fit parameters for the nearby, ESSENCE, and SNLS SNe Ia discussed here.

### 4.1. ESSENCE SN Ia Sample

For the ESSENCE project we find that using photometric selection criteria based on the color and rise time of the candidate object, similar to those used by the SNLS (Howell et al. 2005; Sullivan et al. 2006a), and in good weather and seeing conditions, 80% of the candidates spectroscopically investigated are SNe Ia. We use a deterministic analysis (Blondin & Tonry 2007), as described by Miknaitis et al. (2007), to determine final types and redshifts for our SNe and to cull objects that are not SNe Ia from our sample. All of the ESSENCE supernovae used in this analysis were spectroscopically confirmed as SNe Ia.

During the interval 2002–2005, the ESSENCE project discovered and spectroscopically confirmed 113 SNe Ia. As discussed by Miknaitis et al. (2007), which gives details of these SNe Ia including their celestial coordinates, only 4 of the 15 SNe Ia from 2002 have been fully analyzed, leaving us with 102 SNe Ia. Although we kept SN 1991T–like SNe Ia such as d083, d085, and d093, we rejected the peculiar SN Ia d100 (Matheson et al. 2005). Three SNe Ia were rejected from the nearby+ESSENCE fits because they were at redshifts greater than 0.67 (see below). After we applied the cuts in Tables 1 and 2, we were left with 57 and 60 SNe Ia for MLCS2k2 and SALT, respectively.

With the MLCS2k2 fitter, the largest cut was the 32 SNe Ia rejected because they had fewer than eight data points with $S/N > 5$, no such points after +9 days, or no such points before +4 days. Two of the 102 SNe Ia were located near edges of the detector field of view that we later determined were photometrically less reliable. Due to high $\chi^2$/dof or related poor light-curve goodness-of-fit values, we eliminated an additional six SNe Ia. This left us with a total of 57 ESSENCE SNe Ia for our main MLCS2k2 nearby+ESSENCE analysis. The SALT fitter successfully fitted three more SNe Ia than MLCS2k2, but, in general, our SALT quality cuts accepted the same SNe Ia as our MLCS2k2 quality cuts. The requirements we imposed here on the light curves were stringent cuts to ensure reliable fit pa-

rameters. We are currently engaged in an active program to improve the sensitivity of SN Ia light-curve fitters, and we anticipate recovering ~50% of the SNe Ia rejected here in the final ESSENCE analysis.

### 4.2. Nearby SN Ia Sample

The SN Ia cosmological measurement is fundamentally a comparison of the luminosity distance versus redshift relation at low redshift and high redshift. The ESSENCE SNe Ia alone provide a homogeneous set of luminosity distance versus redshift measurements covering the redshift range $0.15 < z < 0.7$. We selected our nearby SNe Ia from the set compiled by Jha et al. (2007). We applied the light-curve criteria from Tables 1 and 2 and also rejected known peculiar SNe Ia such as SN 2000cx (Li et al. 2001) and SN 2002cx (Li et al. 2003; Jha et al. 2006a). Our list of nearby SNe Ia has 41 SNe Ia in common with the set used by A06. To minimize complications from loosely constrained local peculiar and coordinated flows, we only considered SNe Ia with CMB-frame redshifts of $z > 0.015$. Our final sample consists of 45 nearby SNe Ia as listed in the fit parameter tables (Tables 4 and 5). We used the rederived Landolt/Vega calibration of A06 to determine the passbands for this set of nearby SNe Ia. The light curves we used for these SNe Ia are also included with the ESSENCE light curves available on our Web site (see footnote 21).

### 4.3. External Constraints

To provide complementary cosmological constraints on our SN Ia observations, we include external information from BAOs (Eisenstein et al. 2005). The BAO constraints on ($\Omega_M$, $w$) from Eisenstein et al. (2005) are the most complementary measurement in the ($\Omega_M$, $w$)-plane to our SN Ia measurements, relying only on the observed redshift and angular size of the first acoustic peak in the CMB and not on $H_0$. In addition, because the BAO constraints on $\Omega_M$ are similar in precision (and value) to those derived from large-scale structure (Percival et al. 2001, 2002), from WMAP directly (Spergel et al. 2007), and from the study of X-ray clusters (for a review see Voit 2005), we choose to combine our results only with the BAO results.

We compare the specific model of a flat universe with either $w = -1$ or constant $w$ of any value to our data. SNe Ia have very little leverage on the global flatness of the universe because to first order they measure the difference between $\Omega_M$ and $\Omega_\Lambda$, and flatness depends on the sum. Eisenstein et al. (2005) have constrained curvature to be within $\Omega_K = \pm 0.01$ of flat. The results presented here (from the SNe Ia) on $w$ are not significantly affected by variation of $\Omega_K$ by this amount because the effects of curvature are not noticeable until looking back to much higher redshift. However, nonflat models will significantly alter the BAO results on ($\Omega_M$, $w$) and therefore our joint constraints as well.

For our analysis of only the ESSENCE and nearby SNe Ia, we have chosen to additionally limit our redshift range to $z < 0.670$ to avoid using the rest-frame $U$ band. Since this removes just three ESSENCE SNe Ia from our sample, the trade-off is worthwhile to minimize this source of uncertainty (see § 2). When we include the SNLS or Riess et al. (2004) gold samples, we relax this constraint to incorporate those higher redshift SNe Ia.

In Figures 8 and 9 we show Hubble diagrams of the nearby, ESSENCE, and SNLS samples for the two different fitters we consider in this paper. We overplot an empty universe ($\Omega_M$, $\Omega_\Lambda$) = (0, 0), a matter-only open universe ($\Omega_M$, $\Omega_\Lambda$) = (0.3, 0), and a $\Lambda$CDM concordance cosmology (0.27, 0.73, $-1$). The residuals

---

[23] See http://qold.astro.utoronto.ca/conley/simple_cosfitter/.

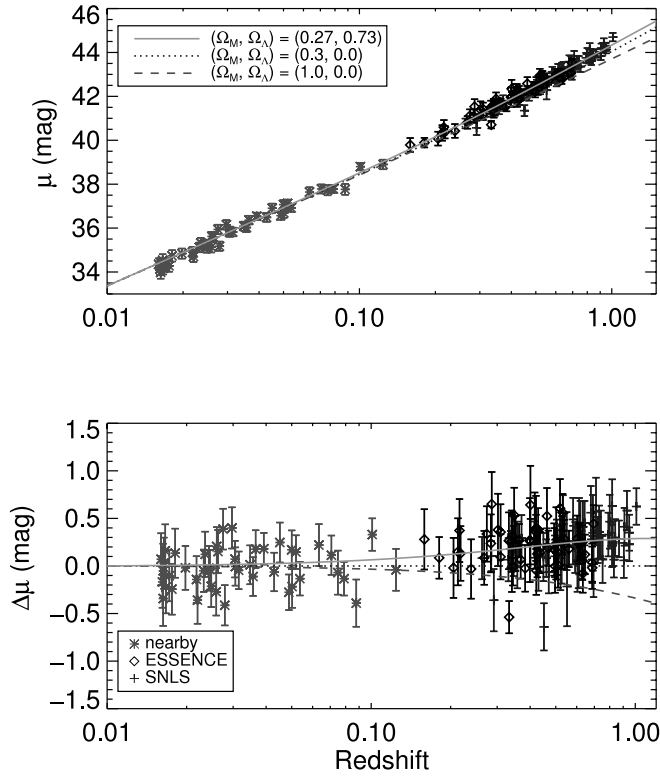FIG. 8.—Relative luminosity distance modulus vs. redshift for the ESSENCE, SNLS, and nearby SNe Ia for MLCS2k2 with the glosz $A_V$ prior. For comparison, the overplotted solid line and residuals are for a $\Lambda$CDM ($w$, $\Omega_M$, $\Omega_\Lambda$) = ($-1$, 0.27, 0.73) universe. [*See the electronic edition of the Journal for a color version of this figure.*]

FIG. 9.—Relative luminosity distance modulus vs. redshift for the ESSENCE, SNLS, and nearby SNe Ia for SALT. For comparison, the overplotted solid line and residuals are for a $\Lambda$CDM ($w$, $\Omega_M$, $\Omega_\Lambda$) = ($-1$, 0.27, 0.73) universe. [*See the electronic edition of the Journal for a color version of this figure.*]

in luminosity distance are then shown with respect to the $\Lambda$CDM model. MLCS2k2 appears to be more suited for the ESSENCE data sample than SALT, although the latter benefits from its flux-based fitting by being able to extract useful luminosity distances from a few more SNe Ia. One SN Ia, d083, is a particular outlier in both fitters at ~0.5 mag brighter than expected in the best-fit or $\Lambda$CDM cosmologies. Matheson et al. (2005) found the spectrum of this object to be like that of SN 1991T, which is the prototype of overluminous SNe Ia. This SN Ia is likely an interesting object worthy of further study and is potentially similar to a similarly superluminous object, SN 2003fg, found in the SNLS survey (Howell et al. 2006). However, given that our sample comprises 60 objects, we certainly allow for the reasonable statistical possibility of a 3 $\sigma$ outlier such as d083 and thus retain it in our sample.

In Figure 10 we show the 1, 2, and 3 $\sigma$ probability contours for our measurement of $w$ versus $\Omega_M$ for ESSENCE+nearby alone, the BAO constraints from Eisenstein et al. (2005), and the combination of the SN Ia and BAO constraints.

Table 9 shows the cosmological parameters $w$ and $\Omega_M$ for each of these sets for flat models of the universe with a constant $w$, as well as the $\chi^2$/dof for a concordance cosmology and the one-dimensional (1D) marginalized values. We detail the calculation of our systematic uncertainties in § 3, present a quantitative summary in Table 7, and arrive at a quadrature sum total of $\Delta w = 0.13$. A $\Lambda$CDM model of the universe fits the MLCS2k2-analyzed ESSENCE+nearby sample with a $\chi^2$/dof of 0.96 and a residual standard deviation of 0.20 mag. Thus, while the estimated $w$ parameter in the constant-$w$ models is $w = -1.05^{+0.13}_{-0.12}$ (stat 1 $\sigma$) $\pm$ 0.13 (sys), a flat, $w = -1$ model of the universe is consistent with our data.
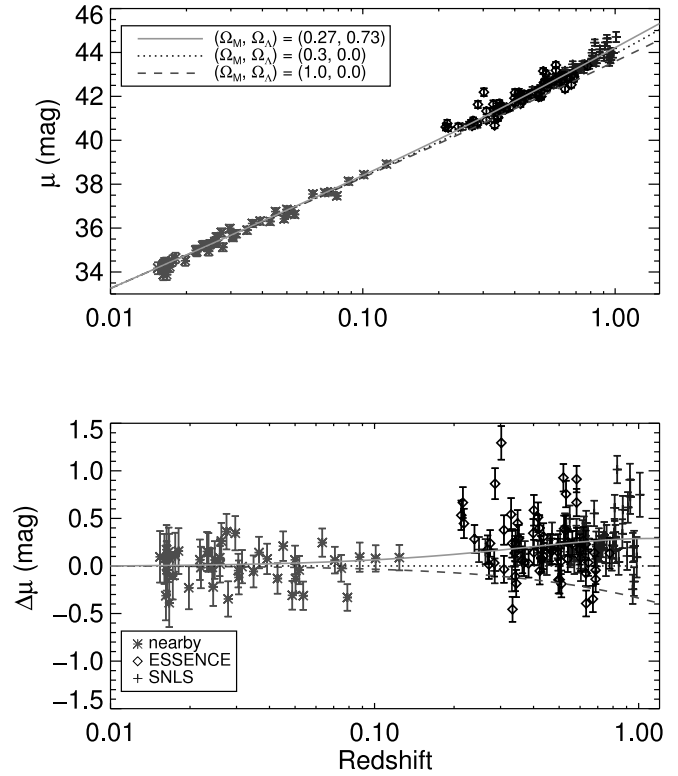
Our results from these 60 SNe Ia from the ESSENCE survey are consistent with the results of A06. It is reassuring that two independent teams using different telescopes and studying different regions of the sky find that SNe Ia at high redshift exhibit the same luminosity distance versus redshift relationship. These samples strengthen and extend the evidence from SNe Ia for dark energy and, together with complementary constraints on $\Omega_M$, point toward simple $\Lambda$CDM models for our universe.

### 4.4. *Joint ESSENCE+SNLS Cosmological Constraints*

A new opportunity presents itself with the release of the SNLS light curves from A06 and the light curves presented in this paper. For the first time it is possible to do a proper, self-consistent joint fit of two large, independent sets of distant SNe Ia.

When fitting the SNLS SNe Ia with MLCS2k2 and the glosz prior, we shift the assumed $A_V$ and $\Delta$ prior selection window functions by $\Delta z = +0.20$ to represent the greater depth of the SNLS survey. The proper way to derive this prior for SNLS would be to model the SNLS survey efficiency and fit simulated SNe Ia with MLCS2k2 as we presented in § 2.3 for the ESSENCE survey. Similar concerns apply for possible selection effects in the heterogeneous nearby sample. Nevertheless, we believe that our use of the glosz prior is appropriate for the low-redshift sample (where it is just the glos prior) and the simple extension in redshift to be a reasonable approach for the SNLS sample. The additional systematic errors introduced by this joint comparison center on the photometric calibration of the distant sample relative to the nearby SNe Ia. We estimate that uncertainty to be the same as the calibration uncertainty to the nominal Vega system used by each project: $\Delta$ zpt = 0.02 mag. We have not modeled different offsets between the two data sets,
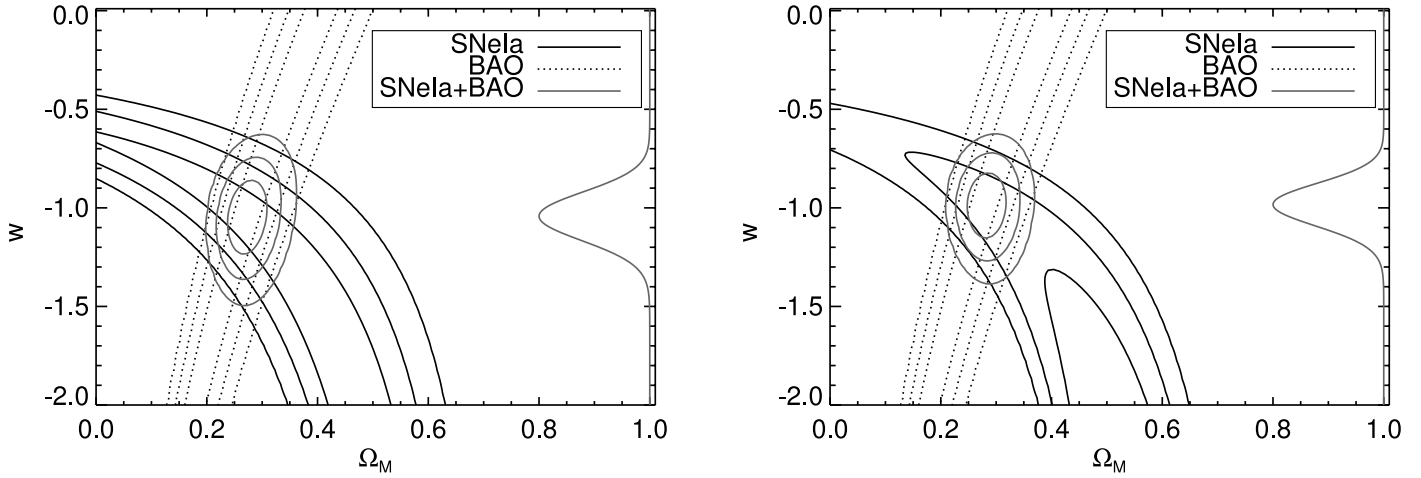
Fig. 10.—The $\Omega_M - w$ 1, 2, and 3 $\sigma$ contours from the ESSENCE+nearby sample for MLCS2k2 with the glosz $A_V$ prior and with the SALT fitter. The BAO constraints are from Eisenstein et al. (2005). [*See the electronic edition of the Journal for a color version of this figure.*]

but we merely express the uncertainty as an additional uncertainty in our inferred cosmological parameters. This relative zero-point uncertainty adds an additional $\Delta w = 0.02$ to our overall systematic uncertainty on $w$.

With our combined analysis, we start with the traditional $\Omega_M - \Omega_\Lambda$ contour plot that was the first clear evidence for dark energy (Riess et al. 1998; Perlmutter et al. 1999).

Table 10 shows the cosmological parameters $w_0$ and $\Omega_M$ for each of these sets for flat models of the universe with a constant $w$, as well as the $\chi^2/\text{dof}$ for a concordance cosmology. A $\Lambda$CDM model of the universe fits the SNLS+ESSENCE+nearby sample analyzed using MLCS2k2 glosz with a $\chi^2/\text{dof}$ of 0.90 from 162 SNe Ia and a residual standard deviation of 0.23 mag. A joint analysis of the luminosity distances from the SALT fitter results in a $\chi^2/\text{dof}$ of 2.76 from 178 SNe Ia and a residual standard deviation of 0.28 mag. This surprisingly larger $\chi^2/\text{dof}$

for the SALT fitter can be seen in the larger number of outliers as visible in a comparison of Figures 8 and 9.

Figure 11 shows the joint MLCS2k2 and SALT results for this joint sample. The estimated $w$ parameter in the constant-$w$ models is $w = -1.07^{+0.09}_{-0.09}$ (stat 1 $\sigma$) $\pm$ 0.13 (sys), and a flat, $w = -1$ model of the universe remains consistent with the current generation of SN Ia data.

### 4.5. *Joint ESSENCE+SNLS+Riess Gold Sample Cosmological Constraints*

In order to explore models with varying $w$, we now include the gold sample from Riess et al. (2004) to extend our reach out to $z \approx 1.5$. The high-quality intermediate-redshift samples of the ESSENCE and SNLS surveys provide an excellent complement to the high-redshift SNe Ia in this set. The heterogeneous nature of the collection of SNe Ia in the gold sample makes it beyond the

TABLE 9
Cosmological Parameters from ESSENCE+Nearby and BAO Constraints

| Sample | Number of SNe Ia[a] | $\Lambda$CDM[b] $\chi^2/\text{dof}$ | Flat, Constant-$w$ (Marginalized 1D) | | |
| --- | --- | --- | --- | --- | --- |
| | | | $\chi^2/\text{dof}$ | $w_0$ | $\Omega_M$ |
| MLCS2k2: "glosz" | | | | | |
| All ESSENCE+nearby............... | 102 | 0.96 | 0.96 | $-1.047^{+0.125}_{-0.124}$ | $0.274^{+0.032}_{-0.020}$ |
| ESSENCE only........................... | 57 | 0.88 | 0.91 | . . . | . . . |
| Nearby only ............................... | 45 | 1.00 | 1.01 | . . . | . . . |
| SALT | | | | | |
| All ESSENCE+nearby............... | 106 | 2.62 | 2.66 | $-0.988^{+0.110}_{-0.109}$ | $0.284^{+0.031}_{-0.020}$ |
| ESSENCE only........................... | 60 | 4.64 | 4.72 | . . . | . . . |
| Nearby only ............................... | 46 | 1.01 | 1.04 | . . . | . . . |

Notes.—The ESSENCE cosmological results given here are for our favored MLCS2k2 "glosz" $A_V$ prior and the SALT fitter of Guy et al. (2005). The dof for the $\Lambda$CDM model is the number of SNe Ia in each set minus the one fit parameter, $\mathcal{M}$. The dof for the best-fit model is the number of SNe Ia minus the three fit parameters $(w, \Omega_M, \mathcal{M})$. For the subsets, the same cosmological fit is used but $\mathcal{M}$ is allowed to float. The $\chi^2/\text{dof}$ for $\Lambda$CDM for the nearby set is 1 by construction. The appropriate additional $\sigma_\mu$ to add in quadrature to recover the full intrinsic dispersion of SNe Ia is determined by requiring $\chi^2/\text{dof}$ of the nearby set to be 1 for $\Lambda$CDM with an assumed peculiar velocity of 400 km s$^{-1}$. The value for $w_0$ is marginalized over $\Omega_M$ assuming a flat, $\Omega_M + \Omega_\Lambda = 1$ universe. Note that the $\chi^2/\text{dof}$ values for the marginalized 1D values are higher than the $\Lambda$CDM model. This is possible because the mean marginalized 1D values are not the points of lowest $\chi^2$. This indicates that there is no reason to favor the marginalized 1D values over the $\Lambda$CDM model.
[a] $0.015 < z$.
[b] $\Lambda$CDM refers to a universe with $(w, \Omega_M, \Omega_\Lambda) = (-1, 0.27, 0.73)$.

TABLE 10
Joint Cosmological Parameters from ESSENCE+SNLS+Nearby and BAO Constraints

| | | $\Lambda$CDM[b] | Flat, Constant-$w$ (Marginalized 1D) | | |
|---|---|---|---|---|---|
| Sample | Number of SNe Ia[a] | $\chi^2$/dof | $\chi^2$/dof | $w_0$ | $\Omega_M$ |
| MLCS2k2: "glosz" | | | | | |
| All ESSENCE+SNLS+nearby............ | 162 | 0.90 | 0.91 | $-1.069^{+0.091}_{-0.093}$ | $0.267^{+0.028}_{-0.018}$ |
| ESSENCE only........................ | 60 | 0.91 | 0.93 | ... | ... |
| SNLS only ........................... | 57 | 0.82 | 0.82 | ... | ... |
| Nearby only .......................... | 45 | 0.99 | 1.01 | ... | ... |
| SALT | | | | | |
| All ESSENCE+SNLS+nearby............ | 178 | 2.76 | 2.79 | $-0.958^{+0.088}_{-0.090}$ | $0.288^{+0.029}_{-0.019}$ |
| ESSENCE only........................ | 64 | 4.77 | 4.78 | ... | ... |
| SNLS only ........................... | 68 | 2.07 | 2.12 | ... | ... |
| Nearby only .......................... | 46 | 0.99 | 1.02 | ... | ... |

Notes.—See notes for Table 9. We include the full sample here without the redshift cut of the ESSENCE-only analysis to consistently include all of the usable SNe Ia.
[a] $z > 0.015$.
[b] $\Lambda$CDM refers to a universe with $(w, \Omega_M, \Omega_\Lambda) = (-1, 0.27, 0.73)$.

scope of this paper to produce definite estimates of the systematic errors that result from including this additional set, but it is tempting to add these SNe Ia and examine the new constraints on cosmological parameters.

We used the 39 nearby SNe Ia in common between the nearby SN Ia sample we discuss here and the gold sample to normalize the luminosity distances between the two sets. To avoid double counting of SNe Ia in this joint analysis, we then drop the nearby SNe Ia from the gold sample and use only the nearby SNe Ia fitted in this paper.

We first compute the $\Omega_M - \Omega_\Lambda$ contours to update the case for dark energy from SNe Ia. Figure 12 represents the most stringent demonstration to date of the existence of dark energy. Independent $\chi^2$ hypothesis testing demonstrates that the SN Ia data alone rule out at $\geq 4.5\ \sigma$ level each an empty universe, an $(\Omega_M, \Omega_\Lambda) = (0.3, 0)$ universe, or an $(\Omega_M, \Omega_\Lambda) = (1, 0)$ universe. The joint constraints on constant-$w$ models from this full set are $w = -1.09^{+0.09}_{-0.10}$. The highest redshift data do not noticeably improve constraints for these models over the set of intermediate-redshift SNe Ia from ESSENCE+SNLS.

It is for models with variable $w$ that the high-redshift data summarized by Riess et al. (2004) provide the most utility. We here provide the global constraints on models characterized by $w = w_0 + w_a(1 - a)$ (Chevallier & Polarski 2001; Linder 2003; Albrecht et al. 2006). Using the BAO constraints on variable $w$ models would require integration from $z = 0.35$ to $z \approx 1089$ and the corresponding assumption that $w = w_0 + w_a(1 - a)$ is the proper parameterization over this stretch. If one is willing to make this assumption, then BAO+CMB already places significant constraints on the allowed $(w_0, w_a)$ parameter space. However, given that our multivariable parameterizations of $w$ are arbitrary models with no clear theoretical motivation, we instead choose to regard $w = w_0 + w_a(1 - a)$ as a local expansion valid out to a redshift of $\sim 2$ but not necessarily to $z \approx 1089$. We then explicitly assume $\Omega_M = 0.27 \pm 0.03$. Figure 13 shows the $(w_0, w_a)$ contours for this combined analysis. Figure 14 represents the region covered in relative distance modulus by the 68% confidence region of the $(w_0, w_a)$ fits in Figure 13. These constraints represent the advances of our understanding of dark energy, but it is clear that work remains to constrain models of variable $w$.
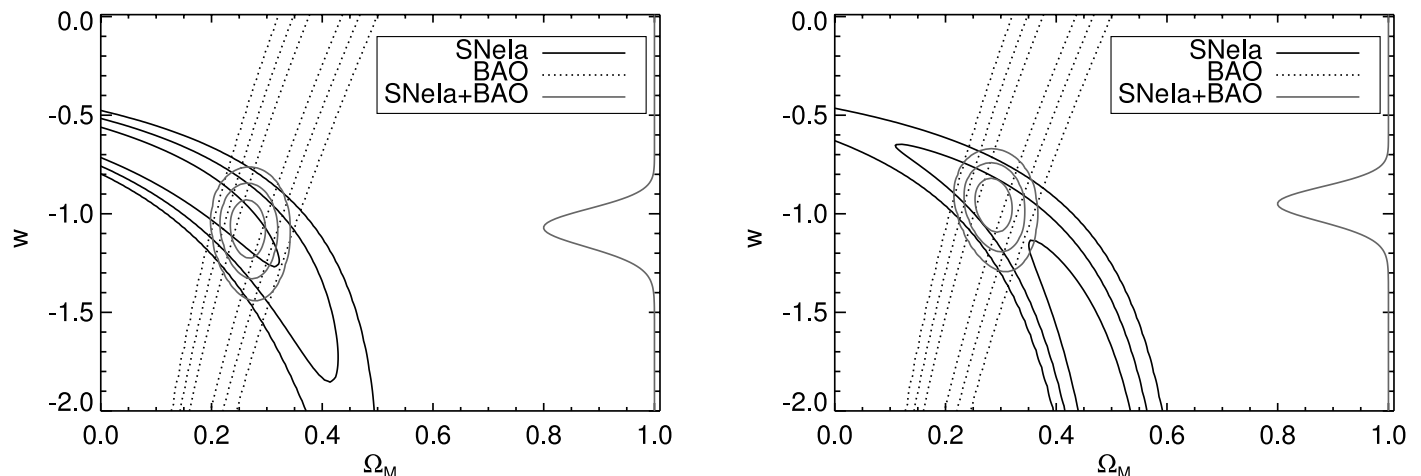


Fig. 11.—The $\Omega_M - w$ contours from the SNLS+ESSENCE+nearby sample for MLCS2k2 with glosz $A_V$ prior and for the SALT fitter. The BAO constraints are from Eisenstein et al. (2005). [See the electronic edition of the Journal for a color version of this figure.]
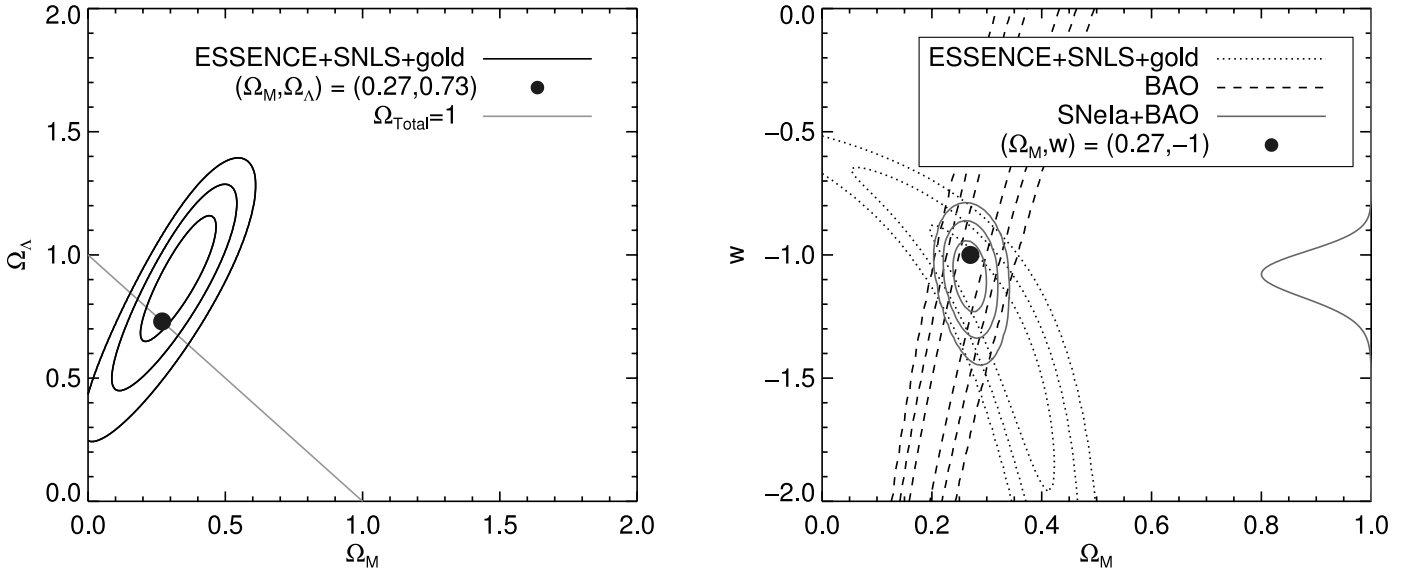
FIG. 12.—SN Ia $(\Omega_M, \Omega_\Lambda)$ and $(\Omega_M, w)$ contours from combining the MLCS2k2 luminosity distances for the ESSENCE SNe Ia analyzed here with the nearby SNe Ia, the SNLS SNe Ia, and the Riess gold sample. The diagonal line in the $(\Omega_M, \Omega_\Lambda)$ plot represents a flat universe, $\Omega_{\text{total}} = \Omega_M + \Omega_\Lambda = 1$. From the SN Ia data alone, an empty universe is ruled out at 4.5 $\sigma$, an $(\Omega_M, \Omega_\Lambda) = (0.3, 0)$ universe at 10 $\sigma$, and an $(\Omega_M, \Omega_\Lambda) = (1, 0)$ universe at >20 $\sigma$. The best combination of data will come after a complete analysis of the calibration and systematic errors of all the data sets. We offer this interim result to indicate the potential of combining low-$z$, ESSENCE, and $z > 1$ SNe Ia. [*See the electronic edition of the Journal for a color version of this figure.*]

In a separate paper (Davis et al. 2007) we extend this analysis to investigate what bounds the current SN Ia data, including the updated gold sample of Riess et al. (2007), can place on a wider range of nonstandard cosmological models, and using model comparison statistics, we conclude that the flat cosmological constant model is still preferred.

## 5. CONCLUSIONS

The ESSENCE survey has successfully discovered, confirmed, and followed 119 SNe Ia in our first 4 years of operation.

We presented results from an analysis of 60 of those SNe Ia here, chosen so as to maximize insight while minimizing susceptibility to systematic errors. We have expended considerable effort to make quantitative estimates of various sources of systematic uncertainty that may afflict the ESSENCE results; of these, host galaxy extinction and a potential local velocity monopole are currently the predominant concerns. We are working to



FIG. 13.—Combined constraints on $(w_0, w_a)$ using the MLCS2k2 luminosity distances for the ESSENCE SNe Ia analyzed here in combination with the nearby SNe Ia, the SNLS SNe Ia, and the Riess gold sample. Here we are considering a two-parameter representation of the dark energy equation-of-state parameter, $w = w_0 + w_a(1 - a)$. Instead of the BAO constraints, we have simply taken $\Omega_M = 0.27 \pm 0.03$. (See cautionary note from Fig. 12.) [*See the electronic edition of the Journal for a color version of this figure.*]



FIG. 14.—Hubble diagram of global SN Ia sample with 68% confidence region of the $w = w_0 + w_a(1 - a)$ models fitted in Fig. 13. [*See the electronic edition of the Journal for a color version of this figure.*]

devise ways to better estimate extinction, using both spectroscopic and photometric observations. Ideally, we would use all available information to arrive at an extinction prior customized for each supernova (e.g., different priors for elliptical and spiral host galaxies), rather than applying a single prior to the collection of all light curves.

The ESSENCE photometric calibration uncertainties will be reduced by our intensive calibration campaign on the CTIO 4 m telescope in conjunction with the improved calibration of the SDSS southern stripe from the SDSS-II project (Frieman et al. 2004; Dilday et al. 2005). We hope to reduce our overall systematic uncertainty to the 5% level through this improved photometric calibration and an improved external nearby SN Ia sample from KAIT, the Nearby Supernova Factory, CfA, SDSS-II, and the Carnegie Supernova Program to reduce our systematic sensitivity to a potential velocity monopole in the local SN Ia sample.

Combining our SN Ia observations with the BAO results of Eisenstein et al. (2005), we find that a fit of a constant-$w$, flat universe model to our data finds an estimated parameter value of $w = -1.05^{+0.13}_{-0.12}$ (stat 1 $\sigma$) $\pm$ 0.13 (sys) with a $\chi^2/\mathrm{dof} = 0.96$ using our full set analyzed with the MLCS2k2 fitter of Jha et al. (2007). A $w = -1$, flat universe model is consistent with our data. A combined analysis of ESSENCE+SNLS+nearby results in an estimated mean parameter of $w = -1.07^{+0.09}_{-0.09}$ (stat 1 $\sigma$) $\pm$ 0.13 (sys). We have no reliable estimate of the systematic effects involving the SALT fitter, but we take our general systematic uncertainty of 0.13 as representative of the issues currently confronting supernova cosmology.

The statistical increase from the SNe Ia from the entire six-year ESSENCE data set plus improved photometric calibration of our detector and photometric measurements will reduce our statistical uncertainty to 7% and, together with an improvement in our systematic uncertainties to the level of 5%, allow us to surpass our goal of a 10% measurement of a constant $w$ in a flat universe.

Establishing the nature of dark energy is among the most pressing issues in the physical sciences today. The emerging impression that the equation-of-state parameter is close to $w = -1$ makes it difficult to determine whether the underlying physics arises in the particle physics sector or from the classical cosmological constant of general relativity. A value of $w = -1$ is perhaps the least informative possible outcome. In our view, this state of affairs motivates a vigorous effort to push the observational constraints to improve our sensitivity to the value and derivative of $w$ and strongly encourages searching for other indications of new physics, as we may well need another piece to solve the puzzle handed us by nature.

*Facilities:* Blanco (MOSAIC II), CTIO:0.9m (CFCCD), Gemini:South (GMOS), Gemini:Gillett (GMOS), Keck:I (LRIS), Keck:II (DEIMOS, ESI), VLT:Antu (FORS1), VLT:Kueyen (FORS1), Magellan:Baade (IMACS), Magellan:Clay (LDSS2)

## REFERENCES

Abazajian, K., et al. 2005, AJ, 129, 1755
Aguirre, A., & Haiman, Z. 2000, ApJ, 532, 28
Aguirre, A. N. 1999a, ApJ, 512, L19
———. 1999b, ApJ, 525, 583
Albrecht, A., et al. 2006, preprint (astro-ph/0609591)
Altavilla, G., et al. 2004, MNRAS, 349, 1344
Astier, P., et al. 2006, A&A, 447, 31 (A06)
Baade, W., & Zwicky, F. 1934, Proc. Natl. Acad. Sci., 20, 254

Barris, B. J., et al. 2004, ApJ, 602, 571
Bassett, B. A., & Kunz, M. 2004, Phys. Rev. D, 69, 101305
Bessell, M. S., Castelli, F., & Plez, B. 1998, A&A, 333, 231
Blondin, S., & Tonry, J. 2007, ApJ, submitted
Blondin, S., et al. 2006, AJ, 131, 1648
Bohlin, R. C., & Gilliland, R. L. 2004, AJ, 127, 3508
Bonacic, A., Schommer, R. A., Suntzeff, N. B., & Phillips, M. M. 2000, BAAS, 32, 1285

Burstein, D. 2003, AJ, 126, 1849

Burstein, D., & Heiles, C. 1978, ApJ, 225, 40

Cardelli, J. A., Clayton, G. C., & Mathis, J. S. 1989, ApJ, 345, 245

Chevallier, M., & Polarski, D. 2001, Int. J. Mod. Phys. D, 10, 213

Clocchiatti, A., et al. 2006, ApJ, 642, 1

Coil, A. L., et al. 2000, ApJ, 544, L111

Colgate, S. A. 1979, ApJ, 232, 404

Commins, E. D. 2004, NewA Rev., 48, 567

Conley, A., et al. 2006, AJ, 132, 1707

Cooray, A., & Caldwell, R. R. 2006, Phys. Rev. D, 73, 103002

Copin, Y., et al. 2006, NewA Rev., 50, 436

Davis, T. M., Schmidt, B. P., & Kim, A. G. 2006, PASP, 118, 205

Davis, T. M., et al. 2007, ApJ, 666, 716

Dilday, B., et al. 2005, BAAS, 37, 1459

Eisenstein, D. J., et al. 2005, ApJ, 633, 560

Elias-Rosa, N., et al. 2005, in ASP Conf. Ser. 342, 1604–2004: Supernovae as Cosmological Lighthouses, ed. M. Turatto (San Francisco: ASP), 247

Filippenko, A. V. 1997, ARA&A, 35, 309

———. 2001, PASP, 113, 1441

———. 2004, in Measuring and Modeling the Universe, ed. W. L. Freedman (Cambridge: Cambridge Univ. Press), 270

———. 2005a, in ASP Conf. Ser. 332, The Fate of the Most Massive Stars, ed. R. Humphreys & K. Stanek (San Francisco: ASP), 33

———. 2005b, in White Dwarfs: Cosmological and Galactic Probes, ed. E. M. Sion, S. Vennes, & H. L. Shipman (Dordrecht: Springer), 97

Filippenko, A. V., Li, W. D., Treffers, R. R., & Modjaz, M. 2001, in ASP Conf. Ser. 246, Small Telescope Astronomy on Global Scales, ed. B. Paczynski, W.-P. Chen, & C. Lemme (San Francisco: ASP), 121

Filippenko, A. V., et al. 1992a, AJ, 104, 1543

———. 1992b, ApJ, 384, L15

Finkbeiner, D. P., Davis, M., & Schlegel, D. J. 1999, ApJ, 524, 867

Fixsen, D. J., Cheng, E. S., Gales, J. M., Mather, J. C., Shafer, R. A., & Wright, E. L. 1996, ApJ, 473, 576

Fixsen, D. J., Dwek, E., Mather, J. C., Bennett, C. L., & Shafer, R. A. 1998, ApJ, 508, 123

Foley, R. J., Filippenko, A. V., Leonard, D. C., Riess, A. G., Nugent, P., & Perlmutter, S. 2005, ApJ, 626, L11

Frieman, J., et al. 2004, BAAS, 36, 1548

Gallagher, J. S., Garnavich, P. M., Berlind, P., Challis, P., Jha, S., & Kirshner, R. P. 2005, ApJ, 634, 210

Garnavich, P. M., et al. 1998, ApJ, 493, L53

Goldhaber, G., et al. 2001, ApJ, 558, 359

Goobar, A., Bergström, L., & Mörtsell, E. 2002, A&A, 384, 1

Guy, J., Astier, P., Nobili, S., Regnault, N., & Pain, R. 2005, A&A, 443, 781

Guy, J., et al. 2007, A&A, 466, 11

Hamuy, M., Phillips, M. M., Suntzeff, N. B., Schommer, R. A., Maza, J., & Aviles, R. 1996, AJ, 112, 2391

Hamuy, M., Phillips, M. M., Wells, L. A., & Maza, J. 1993, PASP, 105, 787

Hamuy, M., Trager, S. C., Pinto, P. A., Phillips, M. M., Schommer, R. A., Ivanov, V., & Suntzeff, N. B. 2000, AJ, 120, 1479

Hamuy, M., et al. 2006, PASP, 118, 2

Hansen, L., Jorgensen, H. E., & Norgaard-Nielsen, H. U. 1987, Messenger, 47, 46

Hatano, K., Branch, D., & Deaton, J. 1998, ApJ, 502, 177

Hicken, M., et al. 2006, BAAS, 208, 72.04

Holz, D. E., & Linder, E. V. 2005, ApJ, 631, 678

Hook, I. M., et al. 2005, AJ, 130, 2788

Howell, D. A. 2001, ApJ, 554, L193

Howell, D. A., et al. 2005, ApJ, 634, 1190

———. 2006, Nature, 443, 308

Hubble, E. P. 1929, ApJ, 69, 103

Hui, L., & Greene, P. B. 2006, Phys. Rev. D, 73, 123526

Jha, S., Branch, D., Chornock, R., Foley, R. J., Li, W., Swift, B. J., Casebeer, D., & Filippenko, A. V. 2006a, AJ, 132, 189

Jha, S., Riess, A. G., & Kirshner, R. P. 2007, ApJ, 659, 122

Jha, S., et al. 2006b, AJ, 131, 527

Kim, A., Goobar, A., & Perlmutter, S. 1996, PASP, 108, 190

Kim, A. G., Linder, E. V., Miquel, R., & Mostek, N. 2004, MNRAS, 347, 909

Kirshner, R. P. 2002, The Extravagant Universe: Exploding Stars, Dark Energy, and the Accelerating Cosmos (Princeton: Princeton Univ. Press)

Knop, R. A., et al. 2003, ApJ, 598, 102

Kowal, C. T. 1968, AJ, 73, 1021

Krisciunas, K., Hastings, N. C., Loomis, K., McMillan, R., Rest, A., Riess, A. G., & Stubbs, C. 2000, ApJ, 539, 658

Krisciunas, K., et al. 2005, AJ, 130, 2453

Kunz, M., & Bassett, B. A. 2004, preprint (astro-ph/0406013)

Leibundgut, B. 1990, A&A, 229, 1

———. 2001, ARA&A, 39, 67

Leibundgut, B., et al. 1993, AJ, 105, 301

———. 1996, ApJ, 466, L21

Li, C., Holz, D. E., & Cooray, A. 2007, Phys. Rev. D, 75, 103503

Li, W., et al. 2001, PASP, 113, 1178

———. 2003, PASP, 115, 453

Li, W. D., et al. 2000, in AIP Conf. Proc. 522, Cosmic Explosions, ed. S. S. Holt & W. W. Zhang (Melville: AIP), 103

Lidman, C. 2004, Messenger, 118, 24

Lidman, C., et al. 2005, A&A, 430, 843

Linder, E. V. 2003, Phys. Rev. Lett., 90, 091301

Lira, P. 1995, M.S. thesis, Univ. Chile

Mather, J. C., Fixsen, D. J., & Shafer, R. A. 1993, Proc. SPIE, 2019, 168

Mather, J. C., et al. 1990, ApJ, 354, L37

Matheson, T., et al. 2005, AJ, 129, 2352

Ménard, B., & Dalal, N. 2005, MNRAS, 358, 101

Miknaitis, G., et al. 2007, ApJ, 666, 674

Minkowski, R. 1941, PASP, 53, 224

Neill, J. D., et al. 2006, AJ, 132, 1126

Nobili, S., et al. 2005, A&A, 437, 789

Norgaard-Nielsen, H. U., Hansen, L., Jorgensen, H. E., Aragon Salamanca, A., & Ellis, R. S. 1989, Nature, 339, 523

Nugent, P., Kim, A., & Perlmutter, S. 2002, PASP, 114, 803

Östman, L., Goobar, A., & Mörtsell, E. 2006, A&A, 450, 971

Overbye, D. 1999, Lonely Hearts of the Cosmos (Boston: Little, Brown)

Percival, W. J., et al. 2001, MNRAS, 327, 1297

———. 2002, MNRAS, 337, 1068

Perlmutter, S. 2003, Phys. Today, 56, 53

Perlmutter, S., et al. 1995, ApJ, 440, L41

———. 1997, ApJ, 483, 565

———. 1998, Nature, 391, 51

———. 1999, ApJ, 517, 565

Petric, A. O., Telis, G. A., Paerels, F., & Helfand, D. J. 2006, ApJ, 651, 41

Phillips, M. M. 1993, ApJ, 413, L105

Phillips, M. M., Lira, P., Suntzeff, N. B., Schommer, R. A., Hamuy, M., & Maza, J. 1999, AJ, 118, 1766

Phillips, M. M., Wells, L. A., Suntzeff, N. B., Hamuy, M., Leibundgut, B., Kirshner, R. P., & Foltz, C. B. 1992, AJ, 103, 1632

Prieto, J. L., Rest, A., & Suntzeff, N. B. 2006, ApJ, 647, 501

Pskovskii, I. P. 1977, Soviet Astron., 21, 675

Radburn-Smith, D. J., Lucey, J. R., & Hudson, M. J. 2004, MNRAS, 355, 1378

Rapetti, D., Allen, S. W., Amin, M. A., & Blandford, R. D. 2007, MNRAS, 375, 1510

Reindl, B., Tammann, G. A., Sandage, A., & Saha, A. 2005, ApJ, 624, 532

Riello, M., & Patat, F. 2005, MNRAS, 362, 671

Riess, A. G. 2000, PASP, 112, 1284

Riess, A. G., Press, W. H., & Kirshner, R. P. 1995, ApJ, 445, L91

———. 1996, ApJ, 473, 88

Riess, A. G., et al. 1997, AJ, 114, 722

———. 1998, AJ, 116, 1009

———. 1999, AJ, 117, 707

———. 2000, ApJ, 536, 62

———. 2004, ApJ, 607, 665

———. 2007, ApJ, 659, 98

Robaina, A. R., & Cepa, J. 2007, A&A, 464, 465

Rust, B. W. 1974, Ph.D. thesis, Univ. Texas

Schlegel, D. J., Finkbeiner, D. P., & Davis, M. 1998, ApJ, 500, 525 (SFD98)

Schmidt, B. P., et al. 1998, ApJ, 507, 46

Shapley, H. 1919, PASP, 31, 261

Spergel, D. N., et al. 2007, ApJS, 170, 377

Stubbs, C. W., & Tonry, J. L. 2006, ApJ, 646, 1436

Sullivan, M., et al. 2003, MNRAS, 340, 1057

———. 2006a, AJ, 131, 960

———. 2006b, ApJ, 648, 868

Tammann, G. A. 1979, in Scientific Research with the Space Telescope, ed. M. S. Longair & J. W. Warner (NASA: Marshall Space Flight Center), 263

Tonry, J. L., et al. 2003, ApJ, 594, 1

Tripp, R. 1998, A&A, 331, 815

Voit, G. M. 2005, Rev. Mod. Phys., 77, 207

Wang, L., Goldhaber, G., Aldering, G., & Perlmutter, S. 2003, ApJ, 590, 944

White, M. 1998, ApJ, 506, 495

Williams, B. F., et al. 2003, AJ, 126, 2608

Wilson, O. C. 1939, ApJ, 90, 634

Wood-Vasey, W. M., et al. 2004, NewA Rev., 48, 637

Zehavi, I., Riess, A. G., Kirshner, R. P., & Dekel, A. 1998, ApJ, 503, 483